Space Sci Rev (2012) 166:37–70
DOI 10.1007/s11214-011-9833-5

The First Magnetic Fields

Lawrence M. Widrow · Dongsu Ryu · Dominik R.G. Schleicher · Kandaswamy Subramanian · Christos G. Tsagas · Rudolf A. Treumann

Received: 11 October 2010 / Accepted: 14 September 2011 / Published online: 7 October 2011

Abstract We review current ideas on the origin of galactic and extragalactic magnetic fields. We begin by summarizing observations of magnetic fields at cosmological redshifts and on cosmological scales. These observations translate into constraints on the strength and scale magnetic fields must have during the early stages of galaxy formation in order to seed the galactic dynamo. We examine mechanisms for the generation of magnetic fields that operate prior during inflation and during subsequent phase transitions such as electroweak symmetry breaking and the quark–hadron phase transition. The implications of strong primordial magnetic fields for the reionization epoch as well as the first generation of stars are discussed in detail. The exotic, early-Universe mechanisms are contrasted with astrophysical processes that generate fields after recombination. For example, a Biermann-type battery

L.M. Widrow (✉)
Department of Physics, Engineering Physics and Astronomy, Queen's University, Kingston, Ontario, Canada K7L 3N6
e-mail: widrow@astro.queensu.ca

D. Ryu
Department of Astronomy and Space Science, Chungnam National University, Daejeon 305-764, Korea
e-mail: ryu@canopus.cnu.ac.kr

D.R.G. Schleicher
Institut für Astrophysik, Georg-August-Universität, Friedrich-Hund-Platz 1, 37077 Göttingen, Germany
e-mail: dschleic@astro.physik.uni-goettingen.de

K. Subramanian
IUCAA, Pune University Campus, Post Bag 4, Ganeshkhind, Pune 411 007, India
e-mail: kandu@iucaa.ernet.in

C.G. Tsagas
Department of Physics, Aristotle University Thessaloniki, Thessaloniki 54124, Greece
e-mail: tsagas@astro.auth.gr

R.A. Treumann
ISSI, Hallerstrasse 6, 3012 Bern, Switzerland
e-mail: treumann@issibern.ch

can operate in a proto-galaxy during the early stages of structure formation. Moreover, magnetic fields in either an early generation of stars or active galactic nuclei can be dispersed into the intergalactic medium.

Keywords Magnetic fields · Inflation · Early Universe · Quark–hadron transition

There is much to be learned about cosmic magnetic fields. We have a rather sketchy information about the field distribution on the largest scales, and the origin of the magnetic fields remains a mystery.

Alexander Vilenkin 2009

1 Introduction

Magnetic fields are observed in virtually all astrophysical systems, from planets to galaxy clusters. This fact is not surprising since gravitational collapse and gas dynamics, the key processes for structure formation, also amplify and maintain magnetic fields. Moreover, the conditions necessary for a magnetic dynamo, namely differential rotation and turbulence, exist in galaxies, which are the building blocks for large scale structure. The one notable example where magnetic fields are searched for but not yet found is in the surface of last scattering. All this raises an intriguing question: When did the first magnetic fields arise?

Numerous authors have suggested that magnetic fields first appeared in the very early Universe. (For recent reviews, see Grasso and Rubinstein 2001, Widrow 2002). There is strong circumstantial evidence that large scale structure formed from the amplification of linear density perturbations that originated as quantum fluctuations during inflation. It is therefore natural to consider whether quantum fluctuations in the electromagnetic field might similarly give rise to large-scale magnetic fields. Indeed, magnetic fields were almost certainly generated during inflation, the electroweak phase transition, and the quark–hadron phase transition but with what strength and on what scale? More to the point, what happened to these fields as the Universe expanded? Were these early Universe fields the seeds for the magnetic fields observed in present-day galaxies or clusters? And even if not, did they leave an observable imprint on the cosmic microwave background?

Exotic early universe mechanisms for field generation stand in contrast with mechanisms that operate in the post-recombination Universe. There are several ways to generate magnetic fields during the epoch of structure formation. At some level, all mechanisms begin with a battery, a process that treats positive and negative charges differently and thereby drives currents. A Biermann battery, for example, can (in fact *must*) operate during the formation of a proto-galaxy. While angular momentum in proto-galaxies is generated by the tidal torques due to nearby systems, vorticity arises from gasdynamical processes. The same processes almost certainly drive currents and hence generate fields, albeit of small amplitude.

The Biermann battery also operates in compact objects such as accretion disks and stars. Since the dynamical timescales for these systems is relatively short, tiny seed fields are rapidly amplified. The magnetic fields in AGN and/or Pop III stars can be expelled into the proto-galactic medium to provide another source of seed fields for subsequent dynamo action.

In this review, we survey ideas on the generation of magnetic fields. Our main focus is on mechanisms that operate in the early Universe, either during inflation, or during the phase

transitions that follow. We contrast these mechanisms with ones that operate during the early stages of structure formation though we leave the details of those ideas for the subsequent chapter on magnetic fields and the formation of large scale structure. The outline of the chapter is as follows: In Sect. 2, we summarize observational evidence for magnetic fields at cosmological redshifts and on supercluster scales and beyond. In Sect. 3, we discuss the generation of magnetic fields during inflation. We make the case that inflation is an attractive arena for magnetic-field generation but for the fundamental result that electromagnetic fields in the standard Maxwell theory and in an expanding, spatially flat, inflating spacetime are massively diluted by the expansion of the Universe. However, one can obtain astrophysically interesting fields in spatially curved metrics or with non-standard couplings between gravity and electromagnetism. Section 4 addresses the question of whether fields can be generated during a post-inflation phase transition. We will argue that strong fields almost certainly arise but that their scales are limited by the Hubble radius at these early times. Only through some dynamical process such as an inverse cascade (which requires appreciable magnetic helicity) can one obtain astrophysically interesting fields. In Sect. 5 we take, as given, the existence of strong fields from an early Universe phase transitions and explore their impact on the post-recombination Universe. In particular, we discuss the implications of strong primordial fields on the first generation of stars and on the reionization epoch. Finally, in Sect. 6 we briefly review field-generation mechanisms that operate after recombination. A summary and some conclusions are presented in Sect. 7.

2 Cosmological Magnetic Fields Observed

The existence of microgauss fields in present-day galaxies and galaxy clusters is well established. These fields can be explained by the amplification of small seed fields over the 13.7 Gyr history of the Universe. However, there is mounting evidence that microgauss fields existed in galaxies when the Universe was a fraction of its present age. Moreover, there are hints that magnetic fields exist on supercluster scales. Both of these observations present challenges for the seed field hypothesis. In this section, we summarize observational evidence for magnetic fields at early times and on cosmological scales and briefly discuss the implications for the seed field hypothesis.

2.1 Galactic Magnetic Fields at Intermediate Redshifts

Microgauss fields are found in present-day galaxies of all types as well as galaxy clusters (see, for example, Kronberg 1994; Widrow 2002; Carilli and Menten 2002; Kulsrud and Zweibel 2008). Perhaps more significant, at least for our purposes, are observations of magnetic fields in intermediate and high redshift galaxies. For example, Kronberg et al. (1992) found evidence for a magnetized galaxy at a redshift of $z = 0.395$. To be specific, they mapped the rotation measure (RM) across the absorption-line quasar, PKS 1229-021 ($z = 1.038$) and determined the residual rotation measure (RRM—defined to be the observed rotation measure minus the Galactic rotation measure). The RRM was then identified with an intervening galaxy whose magnetic properties were inferred by detailed modelling.

Along similar lines, Bernet et al. (2008) provide a compelling argument for magnetic fields at $z \sim 1.3$. Earlier work by Kronberg (2008) found a correlation between the *spread* in the quasar RM distribution and redshift. The naive expectation is that the spread in the distribution should decrease with redshift. Recall that the polarization angle is proportional to the square of the wavelength; the proportionality constant is what we define as the RM. As

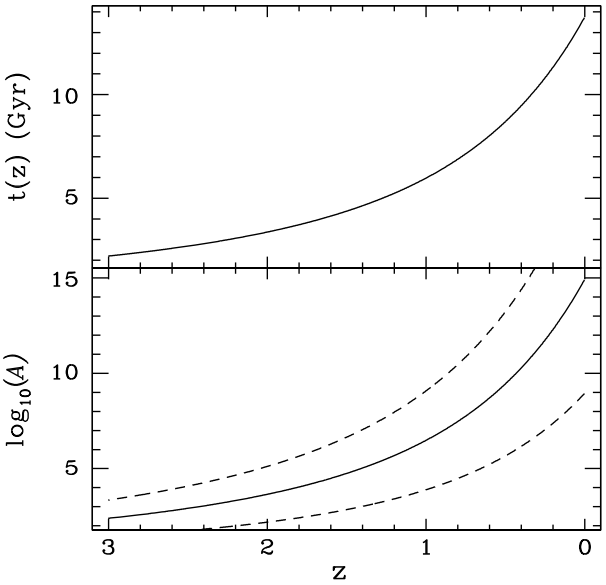

Fig. 1 *Upper panel*: Age of the Universe as a function of redshift for the cosmology described in the text and in Komatsu et al. (2010). *Lower panel*: Amplification factor for a seed magnetic field assuming exponential growth with one of three choices for the growth rate: $\Gamma = 1.5\ \mathrm{Gyr}^{-1}$, $\Gamma = 2.5\ \mathrm{Gyr}^{-1}$ or $\Gamma = 1.5\ \mathrm{Gyr}^{-1}$

electromagnetic radiation propagates from source to observer, the rotation angle is preserved by the wavelength increases as $(1+z)^{-1}$. Hence, the RM is diluted by a factor $(1+z)^{-2}$. In principle, the change in the RM distribution with redshift could be indicative of a redshift dependence in quasar magnetic fields. However, Bernet et al. (2008) sorted the sample according to the presence of MgII absorption lines and showed that the RM spread for set of objects with one or more lines was significantly greater than for the objects with no absorption lines. MgII absorption lines arise as the quasar light passes through the halos of normal galaxies. The implication is that intervening galaxies produce both large RMs and MgII absorption lines and hence, the intervening galaxies must have strong magnetic fields. Simple estimates suggest that the fields are comparable to those in present-day galaxies and that these galaxies are at a redshift of $z \sim 1.3$.

Athreya et al. (1998) studied 15 radio galaxies with redshifts between $z \simeq 2$ and $z \simeq 3.13$ and found significant RM's in almost all of them. Moreover, the RM's were found to differ significantly between the two radio lobes, which suggests that they are due to fields intrinsic to the object rather than due to the Faraday screen of the Galaxy. The RM's, corrected for cosmological expansion and with the Galactic contribution removed, typically range from 100–6000 rad m^{-2}, which implies microgauss fields.

Observations of magnetic fields at intermediate redshift imply a shorter time over which the dynamo can operate. Consider the standard ΛCDM cosmological model with $H_0 = 70.5\ \mathrm{km\,s^{-1}\,Mpc^{-1}}$, $\Omega_m = 0.272$ and $\Omega_\Lambda = 0.728$ where H_0 is the Hubble constant, and Ω_m and Ω_Λ are the density, in units of the critical density, for matter (both baryons and dark matter) and dark energy (Komatsu et al. 2010). In Fig. 1, we show the age of the Universe as a function of redshift for this cosmology. We also show the amplification factor for a seed magnetic field where we assume exponential growth and one of three choices for the growth rate, $\Gamma = 1.5\ \mathrm{Gyr}^{-1}$, $2.5\ \mathrm{Gyr}^{-1}$, or $3.5\ \mathrm{Gyr}^{-1}$. We see that a seed field of only 10^{-21} G is required to reach microgauss strength assuming $\Gamma \simeq 2.5\ \mathrm{Gyr}^{-1}$. However, for the same growth rate, a 10^{-11} G seed field is required to reach microgauss strengths by a redshift $z = 1.3$.

2.2 Magnetic Fields on Supercluster Scales and Beyond

Kim et al. (1989) used the Westerbork Synthesis Radio Telescope to map the Coma cluster and its environs at 326 MHz. Their results provide what remains the best direct evidence for magnetic fields on supercluster scales.

Recently, Neronov and Vovk (2010) argued that the deficit of GeV gamma-rays in the direction of TeV gamma-ray sources yields a *lower bound* of 3×10^{-16} G on the strength of intergalactic magnetic fields. The reasoning goes as follows: TeV gamma-rays and photons from the diffuse extragalactic background light produce $e^{\pm}$ pairs which, in turn, inverse Compton scatter off photons from the cosmic microwave background (CMB). The scattered CMB photons typically have energies in the GeV range. In the absence of appreciable magnetic fields, these secondary photons contribute to the overall emission toward the original TeV source. However, magnetic fields will deflect the intermediate $e^{\pm}$ pairs. Comparison of model predictions with the observed spectrum from HESS Cherenkov Telescopes and upper limits from the NASA Fermi Gamma-Ray Telescope hint at just such a deficit and lead Neronov and Vovk (2010) to derive their lower limit on the magnetic fields. It is important to note that the results of Neronov and Vovk (2010) rely on the assumption that the TeV sources emit gamma-rays continuously for 10^5 years, or longer. This point is stressed in Dermer et al. (2011) who derive a more conservative lower bound of 10^{-18} G based on the assumption that the TeV flux remains constant over the 3–4 year period during which the source has been observed.

Along similar lines, Ando and Kusenko (2010) pointed out that the deflection of $e^{\pm}$ pairs by an intergalactic magnetic field leads to gamma-ray halos around AGN. Indeed, they claim to have found evidence for just such halos in the stacked images of AGN from the Fermi Gamma-ray Telescope and suggested that these halos could be explained by a 10^{-15} Gauss intergalactic magnetic field. Finally, Takahashi et al. (2011) proposed a means to infer the existence of cosmic intergalactic magnetic fields via pair echos from gamma-ray bursts (GRBs). A fraction of the primary gamma-rays from a GRB interact with low-energy photons of the diffuse intergalactic radiation field and produce secondary electron–positron pairs. These pairs produce secondary gamma-rays by inverse Compton upscattering cosmic microwave background (CMB) photons. However, if an intergalactic magnetic field exists, the electrons and positrons will be deflected before interacting with the CMB photons. Thus, the secondary photons will be delayed by an amount that depends on the strength of the magnetic field. Pair echos may be detectable in experiments such as the Cherenkov Telescope Array or the Advanced Gamma-ray Imaging System. Takahashi et al. (2011) suggest that magnetic fields at $z \sim 5$–10 with strength $B \sim 10^{-16}$–10^{-15} G would then produce a measurable effect.

3 Magnetic Fields from Inflation

3.1 General Considerations

The hierarchical clustering scenario provides a compelling picture for the formation of large-scale structure. Linear density perturbations from the early Universe grow via gravitational instability. Small-scale objects form first and merge to create systems of ever-increasing size. The spectrum of the primordial density perturbations, as inferred from the CMB anisotropy spectrum and various statistical measures of large scale structure (e.g., the galaxy two-point correlation function) is generally thought to be scale-invariant and very close to the form

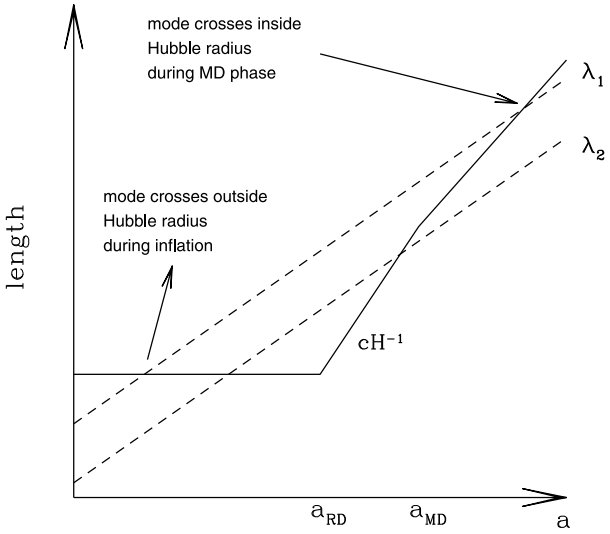

Fig. 2 Evolution of the physical size for the Hubble radius (*solid curve*) and two scales, λ_1 and λ_2 (*dashed curves*) as a function of scale factor a. Shown is the point at which the scale λ_1 crosses outside the Hubble radius during inflation and back inside the Hubble radius during the matter-dominated phase. The scale factors a_{RD} and a_{MD} correspond to the start of the radiation and matter dominated epochs, respectively. Here, λ_1 enters the Hubble volume during the matter-dominated epoch while λ_2 enters the Hubble volume during the radiation-dominated epoch

proposed by Zel'dovich (1970). One of the great successes of inflation is that it leads to just such a spectrum (Guth and Pi 1982; Hawking 1982; Starobinskii 1982). It is therefore natural to ask whether a similar mechanism might generate large-scale magnetic fields.

In order to understand the meaning and significance of the results for density perturbations, we must say a few words about horizons in cosmology. The Hubble radius, essentially, the speed of light divided by the Hubble parameter, sets the maximum scale over which microphysical processes can operate. In a radiation or matter-dominated Universe, the Hubble scale is proportional to the causal scale, that is, the distance over which a photon could have propagated since the Big Bang. The Hubble scale grows linearly with time t in a radiation or matter-dominated Universe. On the other hand, the physical size of an object associated with a fixed comoving (or present-day) scale grows as the scale factor a, which is proportional to $t^{1/2}$ during the radiation-dominated phase and $t^{2/3}$ during the matter-dominated phase. Thus, a physical scale crosses inside the Hubble radius (that is, becomes causally connected) after the Big Bang, with smaller objects crossing earlier than larger ones. This point is illustrated in Fig. 2 and explains why it is so difficult to generate *large-scale* magnetic fields in the early Universe but after inflation.

During inflation, the Hubble parameter is approximately constant (the spacetime is approximately de Sitter) and a physical scale that is initially inside the Hubble radius will cross outside the Hubble radius or Hubble scale, at least until some time later in the history of the Universe (Fig. 2). We therefore have the potential for microphysical processes to operate on large scales during inflation with the consequences of these processes becoming evident much later when the scale re-enters the Hubble radius.

Inflation provides the dynamical means for generating density perturbations: quantum mechanical fluctuations in the de Sitter phase excite modes on the Hubble scale with an energy density set by the Hubble parameter. Therefore, to the extent that the Hubble parameter is constant during inflation, the energy density in modes as they crosses outside the Hubble radius will be scale-independent.

There is one further and crucial part to the story. During inflation, the energy density of the Universe is approximately constant. It is, indeed, the constant energy density that drives the exponential expansion of the de Sitter phase. Naively, we expect the energy density in

(relativistic) fluctuations to scale as a^{-4} and to therefore be diluted by an enormous factor. However, once produced, the fluctuations are stretched to length scales much larger than the Hubble radius. The energy density, $\delta\rho$, in these super-horizon-sized modes is not a gauge invariant quantity in that it depends on ones choice of the surface of simultaneity. However, the quantity $\xi \equiv \delta\rho/(\rho + p)$ is gauge invariant. Moreover, for super-horizon-sized energy density fluctuations, $\xi =$ constant. Thus, the ratio, r, of the energy density in the fluctuation relative to the background density, is the same (up to a constant of order unity) at the time when the mode re-enters the Hubble radius as when it crossed outside the Hubble radius during inflation. This behaviour is often referred to as super-adiabatic growth since it implies that the energy density in the fluctuation grows relative to the energy density in the radiation field.

The equation of motion for a scalar field, ϕ, in a curved spacetime is

$$\nabla^{\alpha}\nabla_{\alpha}\phi - \xi R\phi - \frac{dV}{d\phi} = 0, \tag{1}$$

where R is the Ricci scalar, V is the scalar field potential and ξ is a dimensionless constant. Super-adiabatic growth occurs for a minimally-coupled scalar field ($\xi = 0$). On the other hand, the field evolves adiabatically (energy density scales in the same way as radiation) if it is conformally coupled ($\xi = 1/6$).

The equation of motion for energy density perturbations is identical to that for a minimally coupled scalar field if one ignores the scalar potential term. On the other hand, electromagnetism is conformally-coupled to gravity (at least in the simplest version of the theory). The equation of motion for the gauge field therefore resembles (1) with $\xi = 1/6$. Let us assume that there are de Sitter-induced quantum fluctuations in the electromagnetic field. As with other quantum fields, the energy density of these fluctuations at the time when they are produced, is set by the Hubble parameter. Roughly speaking, $\rho_B \sim H^4$ for modes with physical wavelength $\lambda_{\rm phys} \sim H^{-1}$. Once produced the energy density in these modes scales as a^{-4}, that is, scales in the same way as radiation. Meanwhile, the total energy density of the Universe is constant during inflation and scales as a^{-3} during both the reheating and matter-dominated phases of the Universe. We therefore find that the relative strength a magnetic mode at the end of inflation is

$$\frac{\rho_B}{\rho_t} \simeq 10^{-78}\left(\frac{M}{m_{Pl}}\right)^4\left(\frac{M}{10^{14}\ {\rm GeV}}\right)^{-8/3}\left(\frac{T_{RH}}{10^{10}\ {\rm GeV}}\right)^{-4/3}\left(\frac{\lambda}{\rm Mpc}\right)^{-4}, \tag{2}$$

where λ is the comoving scale of the mode and $m_{Pl} \simeq 10^{19}$ GeV is the Planck mass. The above ratio also depends on the energy scale of our inflation model (M) and on the associated reheating temperature (T_{RH}). During reheating $\rho_B \propto a^{-4}$ and $\rho_t \propto a^{-3}$, which means that $\rho_B/\rho_t \propto a^{-1} \propto T$ between the end of inflation and the radiation era. Therefore, recalling that $\rho_t \simeq M^4$ throughout the de Sitter phase and $\rho_t \simeq \rho_{RH} \simeq T_{RH}^4$ by the end of reheating, expression (2) yields

$$\frac{\rho_B}{\rho_t} \simeq 10^{-104}\left(\frac{\lambda}{\rm Mpc}\right)^{-4}, \tag{3}$$

at the beginning of the radiation epoch (when $\rho_t \simeq \rho_\gamma$). From then on, the high conductivity of the matter is restored and the magnetic flux is conserved (i.e. $B \propto a^{-2}$ and $\rho_B \propto a^{-4}$). As a result, the dimensionless ratio

$$r \equiv \frac{\rho_B}{\rho_\gamma} \simeq 10^{-104}\left(\frac{\lambda}{\rm Mpc}\right)^{-4}, \tag{4}$$

remains constant until today (recall that $\rho_\gamma \propto a^{-4}$ at all times). This result implies a present-day field strength no greater than 10^{-50} G on comoving scales of order 10 kpc, which are the scales relevant for the galactic dynamo.

We are lead to the conclusion that inflation-produced magnetic fields are astrophysically uninteresting. However, this 'negative' result holds for the standard formulation of Maxwell's equations and under the assumption of a spatially-flat FLRW cosmology. In the next sections, we show that super-adiabatic growth can occur in various "open" cosmologies and in models where certain additional couplings between electromagnetism and gravity are included.

3.2 Maxwell's Equations

The Maxwell field may be invariantly described by the antisymmetric Faraday tensor, F_{ab}. Relative to an observer moving with 4-velocity u_a, we can write $F_{ab} = 2u_{[a}E_{b]} + \varepsilon_{abc}B^c$, where $E_a = F_{ab}u^b$ and $B_a = \varepsilon_{abc}F^{bc}/2$ respectively represent the electric and magnetic components of the EM field and ε_{abc} is the 3-dimensional Levi–Civita tensor. Maxwell's equations split into two pairs of propagation and constraint equations (Tsagas 2005). The former consists of

$$\dot{E}_{\langle a\rangle} = -\frac{2}{3}\Theta E_a + (\sigma_{ab} + \omega_{ab})E^b + \varepsilon_{abc}A^b B^c + \mathrm{curl}\, B_a - \mathcal{J}_a, \tag{5}$$

and

$$\dot{B}_{\langle a\rangle} = -\frac{2}{3}\Theta B_a + (\sigma_{ab} + \omega_{ab})B^b - \varepsilon_{abc}A^b E^c - \mathrm{curl}\, E_a, \tag{6}$$

which may be seen as the $1+3$ covariant analogues of the Ampère and the Faraday laws respectively. The constraints, on the other hand, read

$$\mathrm{D}^a E_a = \mu - 2\omega^a B_a \quad \text{and} \quad \mathrm{D}^a B_a = 2\omega^a E_a, \tag{7}$$

providing the $1+3$ forms of Coulomb's and Gauss' laws respectively. In the above Θ, σ_{ab}, ω_{ab} and A_a respectively represent the volume expansion, the shear, the vorticity and the 4-acceleration associated with the observer's motion.[1] In addition, $\mathcal{J}_a$ and μ are the 3-current and the charge densities respectively. We also note that overdots indicate proper-time derivatives and D_a is the 3-dimensional covariant derivative operator. Finally, $\dot{E}_{\langle a\rangle} = h_a{}^b\dot{E}_b$ and $\mathrm{curl}\, B_a = \varepsilon_{abc}\mathrm{D}^b B^c$ by definition, where the tensor h_{ab} projects orthogonal to u_a.

These equations, together with the Einstein equations and the Ricci identities, lead to wave equations for the electric and magnetic fields. For example, linearised on a Friedmann–Lemaître–Robertson–Walker (FLRW) background, the wave equations of the electric and the magnetic components of the Maxwell field read (Tsagas 2005)

$$\ddot{E}_a - \mathrm{D}^2 E_a = -5H\dot{E}_a + \frac{1}{3}\kappa(\rho + 3p)E_a - 4H^2 E_a - \frac{1}{3}\mathcal{R}E_a - \dot{\mathcal{J}}_a - 3H\mathcal{J}_a \tag{8}$$

[1] By construction $\Theta = \mathrm{D}^a u_a$ is the volume scalar, which determines whether we have expansion ($\Theta > 0$), or contraction ($\Theta < 0$). The shear tensor ($\sigma_{ab} = \mathrm{D}_{(b}u_{a)} - (\Theta/3)h_{ab}$) monitors changes in the shape of the fluid element under constant volume, while the vorticity tensor ($\omega_{ab} = \mathrm{D}_{[b}u_{a]}$) governs the rotational behaviour of the medium. Finally, the 4-acceleration, $A_a = \dot{u}_a$, reflects the presence of non-gravitational forces and vanishes when the motion is driven by gravity alone (see Tsagas et al. 2008 for details). Note that the antisymmetry of the vorticity tensor allows us to define the vorticity vector, by means of $\omega_a = \varepsilon_{abc}\omega^{bc}/2$, which also determines the rotational axis.

and

$$\ddot{B}_a - \mathrm{D}^2 B_a = -5H\dot{B}_a + \frac{1}{3}\kappa(\rho + 3p)B_a - 4H^2 B_a - \frac{1}{3}\mathcal{R}B_a + \mathrm{curl}\,\mathcal{J}_a, \tag{9}$$

respectively. Here, $H = \dot{a}/a = \Theta/3$ is the background Hubble parameter, $\mathcal{R} = 6K/a^2$ is the Ricci scalar of the spatial sections (with $K = 0, \pm 1$), $\kappa = 8\pi G$ is the gravitational constant and $\mathrm{D}^2 = \mathrm{D}^a \mathrm{D}_a$ is the 3-D covariant Laplacian. Note the 3-Ricci term, which reflects a purely relativistic/geometrical coupling between the electromagnetic field and the spacetime curvature. We will return to this particular interaction to examine the way it can affect the evolution of cosmological magnetic fields.

3.3 Ohm's Law in the Expanding Universe

The literature contains various expressions of Ohm's law, which provides the propagation equation of the electric 3-current. For a single fluid at the limit of resistive magnetohydrodynamics (MHD), Ohm's law takes the simple form (Greenberg 1971; Jackson 1975)

$$\mathcal{J}_a = \sigma E_a, \tag{10}$$

where σ represents the electric conductivity of the matter (not to be confused with the shear tensor σ_{ab}). In highly conducting environments, $\sigma \to \infty$ and the electric field vanishes. This is the familiar ideal-MHD approximation where the electric currents keep the magnetic field frozen-in with the charged fluid. Conversely, when the conductivity is very low, $\sigma \to 0$. Then, the 3-currents vanish despite the presence of nonzero electric fields. Here, we will consider these two limiting cases. For any intermediate case, one needs a model for the electrical conductivity of the cosmic medium.

3.4 Adiabatic Decay of Magnetic Fields in a Spatially Flat FLRW Cosmology

Consider the case of a poorly conductive environments where there are no 3-currents. The wave equation (9), then reduces to

$$\ddot{B}_a - \mathrm{D}^2 B_a = -5H\dot{B}_a + \frac{1}{3}\kappa(\rho + 3p)B_a - 4H^2 B_a - \frac{1}{3}\mathcal{R}B_a. \tag{11}$$

To simplify the above, we introduce the rescaled the magnetic field $\mathcal{B}_a = a^2 B_a$ and employ conformal time, η, where $\dot{\eta} = 1/a$. Then, on using the harmonic splitting $\mathcal{B}_a = \sum_n \mathcal{B}_{(n)} \mathcal{Q}^{(n)}_a$—so that $\mathrm{D}_a \mathcal{B}_{(n)} = 0 = \dot{\mathcal{Q}}^{(n)}_a = \mathrm{D}^a \mathcal{Q}^{(n)}_a$ and $\mathrm{D}^2 \mathcal{Q}^{(n)}_a = -(n/a)^2 \mathcal{Q}^{(n)}_a$, expression (11) takes the compact form

$$\mathcal{B}''_{(n)} + n^2 \mathcal{B}_{(n)} = -2K\mathcal{B}_{(n)}, \tag{12}$$

with the primes denoting conformal-time derivatives, n representing the comoving wavenumber of the mode and $K = 0, \pm 1$ (Tsagas 2005). Note the magneto-curvature term in the right-hand side of (12), which shows that the magnetic evolution also depends on the spatial geometry of the FLRW spacetime.

When the background has Euclidean spatial hypersurfaces, the 3-curvature index is zero (i.e. $K = 0$) and expression (12) assumes the Minkowski-like form

$$\mathcal{B}''_{(n)} + n^2 \mathcal{B}_{(n)} = 0. \tag{13}$$

This equation accepts the oscillatory solution $\mathcal{B}_{(n)} = C_1 \sin(n\eta) + C_2 \cos(n\eta)$, which recasts into

$$B_{(n)} = \left[\mathcal{C}_1 \sin(n\eta) + \mathcal{C}_2 \cos(n\eta)\right]\left(\frac{a_0}{a}\right)^2, \tag{14}$$

for the actual B-field. In other words, the adiabatic ($B_{(n)} \propto a^{-2}$) depletion of the magnetic component is guaranteed, provided the background spacetime is a spatially flat and the electrical conductivity remains very poor. Applied during inflation, this result leads to (2).

The adiabatic decay-law also holds in highly conductive environments. There, $\sigma \to \infty$ and, according to Ohm's law (see (10)) the electric field vanishes in the frame of the fluid. As a result, Faraday's law (see (6)) linearises to

$$\dot{B}_a = -2H B_a, \tag{15}$$

around an FLRW background. The above ensures that $B_a \propto a^{-2}$ on all scales, regardless of the equation of state of the matter and of the background 3-curvature. Applied after inflation and combined with (3), this result leads directly to (4).

3.5 Superadiabatic Magnetic Amplification in Spatially Open FLRW Models

The "negative" results discussed at the beginning of this section have been largely attributed to the conformal invariance of Maxwell's equations and to the conformal flatness of the Friedmannian spacetimes. The two are thought to guarantee an adiabatic decay-rate for all large-scale magnetic fields at all times. Equation (14), however, only holds for the spatially flat FLRW cosmology. Although all three FLRW universes are conformally flat, only the spatially flat model is globally conformal to Minkowski space. For the rest, the conformal mappings are local. Put another way, in spatially curved Friedmann universes, the conformal factor is no longer the cosmological scale factor but has an additional spatial dependence (e.g. see Stefani 1990; Keane and Barrett 2000). This means that the wave equation of the rescaled magnetic field ($\mathcal{B}_a = a^2 B_a$) takes the simple Minkowski-like form (13) only on FLRW backgrounds with zero 3-curvature. In any other case, there is an additional curvature-related term (see expressions (11) and (12)), which reflects the non-Euclidean spatial geometry of the host spacetime. As a result, when linearised around an FLRW background with nonzero spatial curvature, the magnetic wave equation (see (12)) reads

$$\mathcal{B}''_{(n)} + \left(n^2 \pm 2\right)\mathcal{B}_{(n)} = 0, \tag{16}$$

where the plus and the minus signs refer to spatially closed and open models, respectively. Recall that in the former case the eigenvalues are discrete (with $n^2 \geq 3$) and in the latter continuous (with $n^2 \geq 0$). As expected, the curvature-related effects fade away as we move to progressively smaller scales (i.e. for $n^2 \gg 2$).

Equation (16) shows that on FLRW backgrounds with spherical spatial hypersurfaces, the B-field still decays adiabatically. The picture changes when the background FLRW model is open. There, the hyperbolic geometry of the 3-D hypersurfaces alters the nature of the magnetic wave equation on large enough scales (i.e. when $0 < n^2 < 2$). These wavelengths include what we may regard as the largest subcurvature modes (i.e. those with $1 \leq n^2 < 2$) and the supercurvature lengths (having $0 < n^2 < 1$). Note that eigenvalues with $n^2 = 1$ correspond to the curvature scale with physical wavelength $\lambda = \lambda_K = a$ (e.g. see Lyth and Woszczyna 1995). Here, we will focus on the largest subcurvature modes.

We proceed by introducing the scale-parameter $k^2 = 2 - n^2$, with $0 < k^2 < 2$. Then, $k^2 = 1$ indicates the curvature scale, the range $0 < k^2 < 1$ corresponds to the largest subcurvature modes and their supercurvature counterparts are contained within the $1 < k^2 < 2$ interval. In the new notation and with $K = -1$, (16) recasts into

$$\mathcal{B}''_{(n)} - k^2 \mathcal{B}_{(n)} = 0, \tag{17}$$

with the solution given by $\mathcal{B}_{(k)} = C_1 \sinh(|k|\eta) + C_2 \cosh(|k|\eta)$. Written in terms of the actual magnetic field, the latter takes the form (Tsagas and Kandus 2005; Barrow and Tsagas 2008)

$$B_{(k)} = \left[\mathcal{C}_1 \mathrm{e}^{|k|(\eta-\eta_0)} + \mathcal{C}_2 \mathrm{e}^{-|k|(\eta-\eta_0)}\right]\left(\frac{a_0}{a}\right)^2. \tag{18}$$

Magnetic fields that obey the above evolution law can experience superadiabatic amplification without modifying conventional electromagnetism and despite the conformal flatness of the FLRW host. For instance, during the radiation era, the scale factor of an open FLRW universe evolves as $a \propto \sinh(\eta)$. Focusing on the curvature length, for simplicity, we may set $|k| = 1$ in (18). On that scale, the dominant magnetic mode never decays faster than $B_{(1)} \propto a^{-1}$. The B-field has been superadiabatically amplified.

Analogous amplification also occurs during the dust and the reheating eras (when $p = 0$ and $a = \sinh^2(\eta/2)$), as well as in open FLRW universes with an inflationary (i.e. $p = -\rho$) equation of state. In fact, the superadiabatic amplification of large-scale magnetic fields is essentially independent of the equation of state of the matter and appears to be a generic feature of the open Friedmann models (see Barrow and Tsagas 2011 for further discussion and details). During slow-roll inflation, in particular, the scale factor evolves as (Tsagas et al. 2008)

$$a = a_0 \left(\frac{1 - \mathrm{e}^{2\eta_0}}{1 - \mathrm{e}^{2\eta}}\right)\mathrm{e}^{\eta-\eta_0}, \tag{19}$$

where $\eta, \eta_0 < 0$. Substituting the above into (18), we find that near the curvature scale (i.e. for $|k| \to 1$) the magnetic evolution is given by

$$B_{(1)} = \mathcal{C}_3\left(1 - \mathrm{e}^{2\eta}\right)\left(\frac{a_0}{a}\right) + \mathcal{C}_4 \mathrm{e}^{-\eta}\left(\frac{a_0}{a}\right)^2, \tag{20}$$

with $\mathcal{C}_3$, $\mathcal{C}_4$ depending on the initial conditions. This also implies superadiabatic amplification for the B-field, since the dominant mode never decays faster than $B_{(1)} \propto a^{-1}$. The adiabatic decay rate is only recovered at the end of inflation, as $\eta \to 0$.[2]

The strength of the residual magnetic strength is calculated in a way analogous to that given in the previous section. This time, however, the B-field has been superadiabatically amplified throughout the lifetime of the universe. Then, close to the curvature scale, where $B \propto a^{-1}$, we find that

[2]The magnetogeometrical interaction and the resulting effects are possible because, when applied to spatially curved FLRW models, inflation does not lead to a globally flat de Sitter space. Although the inflationary expansion dramatically increases the curvature radius of the universe, it does not change its spatial geometry. Unless the universe was perfectly flat from the beginning, there is always a scale where the 3-curvature effects are important. It is on these lengths that primordial B-fields can be superadiabatically amplified.

$$r = \frac{\rho_B}{\rho_\gamma} \simeq 10^{-8}\left(\frac{M}{10^{14}\ \mathrm{Gev}}\right)^4\left(\frac{\lambda}{\mathrm{Mpc}}\right)^{-2}$$
$$\simeq 10^{-8}\left(\frac{M}{10^{14}\ \mathrm{GeV}}\right)^4\left(\frac{\lambda_H}{\mathrm{Mpc}}\right)^{-2}(1-\Omega), \tag{21}$$

at present (Barrow and Tsagas 2011). Note that $\lambda \to \lambda_K = \lambda_H/\sqrt{1-\Omega}$, with λ_K, λ_H and Ω representing the curvature scale the Hubble length and the density parameter of the universe respectively. According to (21), the higher the scale of inflation, the stronger the amplification. On the other hand, the larger the curvature scale, namely the higher the number of e-folds during inflation, the weaker the residual magnetic field (see Barrow and Tsagas 2011 for further discussion). Setting $M \sim 10^{14}$ GeV and $\lambda_H \sim 10^3$ Mpc in the right-hand side of (21), we find a current (comoving) magnetic strength of approximately 10^{-14} Gauss on scales close to the present curvature length. The latter is approximately 10^4 Mpc if we assume that $1-\Omega \sim 10^{-2}$ today (Komatsu et al. 2010). These lengths are far larger than 10 kpc; the minimum magnetic size required for the dynamo to work. Nevertheless, once the galaxy formation starts, the field lines should break up and reconnect on scales similar to that of the collapsing protogalactic cloud.

Galactic-scale magnetic fields of strength 10^{-14} G are stronger than those generated by many of the other scenarios considered in the literature (see below) and may be strong enough to seed the galactic dynamo. Recall, however, that inflation was introduced to avoid various shortcomings of the standard cosmological model including the so-called flatness problem. Essentially, inflation is meant to inflate away (push to extremely large scales) any curvature that might exist in the pre-inflationary Universe. Evidently, for superadiabatic growth of magnetic field without explicit conformal symmetry breaking (as described in the next section) one requires enough inflation to push the curvature scale beyond our present Hubble volume, but not too far beyond. To be quantitative, the most recent analysis by the WMAP group (Komatsu et al. 2010) finds that the effective energy density parameter for curvature, $\Omega_K \equiv -K/(aH)^2 = 1-\Omega_\Lambda-\Omega_m$, is constrained between $-0.0133 < \Omega_K < 0.0084$. Should future measurements find Ω_K to be more consistent with negative curvature, rather than zero or positive curvature, they would lend credence to the mechanism for magnetic amplification described above.

3.6 Inflation-Produced Magnetic Fields via Non-conformal Couplings

As pointed out above, the electromagnetic field is conformally coupled to gravity and therefore, in a spatially flat, FLRW cosmology, the magnetic fields generated during inflation decay adiabatically and are therefore of negligible astrophysical importance. Turner and Widrow (1988) pointed out that by adding additional terms to the Lagrangian such as RA^2 and $R_{\mu\nu}A^\mu A^\nu$ one explicitly breaks conformal invariance and can essentially force the magnetic field to behave like a minimally-coupled scalar field. These terms also break gauge invariance and hence induce an effective mass for the photon whose size depends on the spacetime curvature. In fact, the effective mass-squared for the photon is negative for the case where the magnetic field behaves as a minimally-coupled scalar field. A negative mass-squared signals an instability in the semi-classical equations for the field and can be viewed as the origin of the superadiabaticity. Such terms also lead to potential theoretical difficulties in the particle theory and numerous authors have attempted to find more effective and more natural ways to break conformal invariance. Indeed, Turner and Widrow (1988), recognizing the potential for such difficulties, considered terms such as RF^2 which break

conformal invariance but not gauge invariance. They also briefly considered $\varphi F\tilde{F} \sim \varphi \mathbf{E}\cdot\mathbf{B}$ terms where φ was a pseudo-scalar (i.e., axion-like terms). Ratra (1992) demonstrated that appreciable magnetic fields couple be produced during inflation if the electromagnetic field couples to the inflaton field, Φ, through a term of the form $e^{\alpha\Phi}F_{\mu\nu}F^{\mu\nu}$ where α is a constant. In his model, the inflaton potential is also an exponential: $V(\Phi) \propto \exp(-q\Phi)$. An attractive feature of this model is that is preserves gauge invariance since the additional term is constructed from the Maxwell tensor, F, rather than the gauge field, A. Along similar lines Gasperini et al. (1995) demonstrated that magnetic fields of sufficient strength to seed the galactic dynamo could be produced in a string-inspired cosmology. In their model, the electromagnetic field is coupled to the dilaton which, in turn, is coupled to gravity. The dilaton is a scalar field that naturally arises in theories with extra dimensions and whose vacuum expectation value effectively controls Newton's constant.

The RA^2 terms give rise to "ghosts" in the theory which signal an instability of the vacuum (Himmetoglu et al. 2009a, 2009b). A theory with ghosts is internally consistent only as an effective low-energy theory and hence is only valid below some energy scale, Λ. Himmetoglu et al. (2009b) argue that $\Lambda \lesssim$ MeV but this scale is well below the scales assumed in models for inflation-produced magnetic fields. Thus, their results call into question the viability of the mechanism. A detailed and critical analysis of magnetic-field production in string-inspired models of inflation can be found in Martin and Yokoyama (2008) (see, also, the review by Subramanian 2010). There, particular attention was paid to a potential back-reaction problem which arises if the *electric* fields produced along with the magnetic fields have an energy density comparable to the background energy density. Similar conclusions were reached in Demozzi et al. (2009). In models the RA^2 terms, the longitudinal degree of freedom of the **A**-field becomes dynamical. Demozzi et al. (2009) argued that the energy density associated with this component grows during inflation and could, in principle, shut off inflation. Indeed, they found that the magnetic field should not exceed 10^{-32} G on Mpc-scales today. Demozzi et al. (2009) also considered backreaction from F^2 terms and found that interesting magnetic fields required large couplings where perturbation theory could not be trusted. Durrer et al. (2011) studied field generation from $\varphi F\tilde{F}$ terms and found that while backreaction does not appear to be a problem in this scenario, the fields that arose were generally too weak to seed a galactic dynamo. In summary, while inflation remains an attractive arena for the production of seed magnetic fields, there appear to be significant, if not insurmountable, technical difficulties with the scenario.

4 Magnetic Fields from Early Universe Phase Transitions

The early universe was characterized by a series of phase transitions in which the nature of particles and fields changed in fundamental ways (see Fig. 3). For example, electroweak symmetry breaking marked the transition from a high-energy regime in which the W and Z bosons and the photon were effectively massless and interchangeable to one in which the W and Z bosons were heavy while the photon remained massless. The transition also marked the emergence of two distinct forces: electromagnetism and the weak nuclear force. Likewise, the Quark–Hadron phase transition marked the transition from the free quark–gluon phase to one in which quarks were locked into baryons. Both of these transitions had the potential to generate strong magnetic fields since they involved the release of an enormous amount of free energy and since they involve charged particles which could, in turn, drive currents. Indeed, strong magnetic fields are almost certainly generated. The question is one of physical scale since the Hubble radius was so small at these early times.

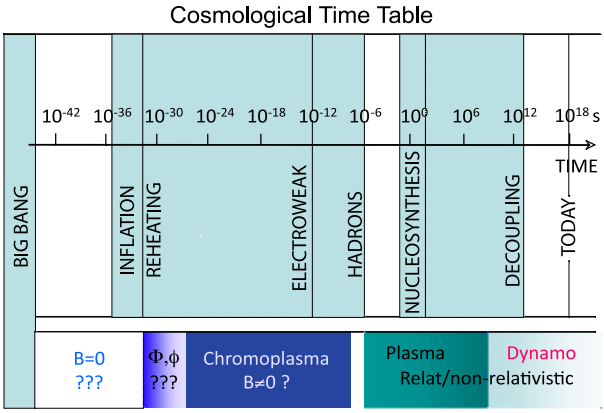

Fig. 3 The cosmological periods. Starting with reheating the quantum chromodynamic quark–gluon–plasma period lasts until hadron formation. Non-Abelian Weibel instabilities may be responsible for generating seed magnetic fields during this time, which in the presence of free energy grow from non-Abelian thermal fluctuations. At later times the period of relativistic and classical plasma sets on. Here seed magnetic fields can be generated from thermal background electrodynamic fluctuations if thermal anisotropies or beams can exist in this regime

4.1 General Considerations

At any phase in the history of the Universe, the strength of the fields generated by some microphysical process is limited by equipartition with the background energy density. Moreover, the maximum scale for magnetic fields generated by a microphysical process is set by the Hubble radius. For a radiation-dominated Universe, the energy density of the Universe is given by $\rho \propto g_* T^4$ where T is the temperature of the thermal bath and g_* counts the effective number of relativistic degrees of freedom (see, for example, Kolb and Turner 1990; Peacock 1999). The Hubble radius is given by $L_H = c/H$ where $H = a^{-1}da/dt \propto T^2$ is the Hubble parameter. Numerically, we have

$$B_{\rm max}\left(l = cH^{-1},\, T\right) = B_{\rm equipartition}(T) \simeq 10^{18}\ {\rm Gauss}\left(\frac{T}{150\ {\rm MeV}}\right)^2 \tag{22}$$

for

$$l \simeq 100\ {\rm cm}\left(\frac{150\ {\rm MeV}}{T}\right)^2. \tag{23}$$

In practice, the strength of fields generated during some early Universe phase transition will be well below the value set by equipartition and have a length scale significantly smaller than the Hubble radius. We therefore write $B(l, T) = f B_{\rm max}$ for $l = gc/H$ and f and g are constants.

Typically, we are interested in fields on scales much larger than the characteristic scales of the original field. On purely geometric grounds, Hogan (1983) argued that the field strength on some large scale L due to small-scale cells of size l with field strength $B(l)$ will be $B(L) = B(l)(l/L)^{3/2}$. However, Durrer and Caprini (2003) showed that the divergence-free nature of the magnetic field places a constraint on the statistical properties of the field and that the most natural choice of scaling is $B(L) = B(l)(l/L)^{5/2}$. Their derivation assumes a scale-free energy spectrum for the magnetic field which may not apply for fields produced

during an early Universe phase transition. Nevertheless, the argument does call into question Hogan's result.

In the absence of some dynamical effect, the field strength will be diluted by the expansion as a^{-2} between the time when it is generated and some later time. Thus, a field $B(l, T)$ generated prior to recombination will lead to a field at recombination with strength

$$B(L, T_{\rm rec}) = B(l, T)\left(\frac{T_{\rm rec}}{T}\right)^2\left(\frac{l}{L}\right)^{\beta} \tag{24}$$

where $\beta = 5/2$, according to Durrer and Caprini (2003). More generally we have the following scaling:

$$B(L, T) \sim f g^{\beta} T^{-\beta} L_{\rm cm}^{-\beta}, \tag{25}$$

where we emphasize that L is the comoving length scale.

4.2 First-Order Phase Transitions

Detailed calculations of magnetic field generation during the electroweak and QCD phase transitions have been carried out by numerous authors. By and large, these groups assume that the transitions are first-order, that is characterized by a mixed-phase regime in which bubbles of the new phase nucleate and expand, eventually filling the volume. The energy associated with the bubble walls is released as a form of latent heat. Quashnock et al. (1989) demonstrated that a Biermann battery can operate during the QCD phase transition. The up, down, and strange quarks (the three lightest quarks) have charges $2/3$, $-1/3$, and $-1/3$ respectively. If these quarks were equal in mass, the quark–gluon plasma would be electrically neutral. However, the strange quark is heavier and therefore less abundant. The implication is that there is a net positive charge in the quark–gluon plasma and a net negative charge in the lepton sector. Electric currents are therefore generated at the bubble walls that separate the quark phase from the baryon phase. Quashnock et al. (1989) found that 5 G fields could be generated on scales of 100 cm at the time of the QCD phase transition. Following the arguments outlined above, the field strength on galactic scales at the time of recombination would be (a disappointingly small) $\sim 10^{-31}$ G.

Somewhat larger estimates were obtained by Cheng and Olinto (1994) and Sigl et al. (1997) who realized that as the hadronic regions grow, baryons would concentrate on the bubble walls due to a "snowplow" effect. (Sigl et al. 1997 also showed that fluid instabilities could give rise to strong magnetic fields during the QCD phase transition.) For reasonable parameters, they obtained fields about seven orders of magnitude larger than those found by Quashnock et al. (1989).

Magnetic fields can arise during cosmological phase transitions even if they are second order—that is, phase transitions signaled by the smooth and continuous transition of an order parameter. Vachaspati (1991), for example, showed that gradients in the Higgs field vacuum expectation value (the order parameter for the electroweak phase transition) induce magnetic fields on a scale $\sim T_{EW}^{-1}$ with strength of order $q_{EW}^{-1} T_{EW}^{-2}$ where T_{EW} is the temperature of the electroweak phase transition and q_{EW} is the Higgs field coupling constant. To estimate the field on larger scales, Vachaspati (1991) assumed that the Higgs field expectation value executed a random walk with step size equal to the original coherence length. The field strengths were small (10^{-23} G on 100 kpc scales) but not negligible.

4.3 Inverse Cascade

The discussion above suggests that strong magnetic fields are likely to have been generated in the early Universe but that their coherence length is so small, the effective large-scale fields are inconsequential for astrophysics. However, dynamical mechanisms may lead to an increase in the coherence length of magnetic fields produced at early times. Chief among these is an inverse cascade of magnetic energy from small to large scales which occurs when there is substantial magnetic helicity (Frisch et al. 1975). The effect was investigated in the context of primordial magnetic fields (see, for example, Cornwall 1997; Son 1999; Field and Carroll 2000; Brandenburg 1996; Banerjee and Jedamzik 2004). As the Universe expands, magnetic energy shifts to large scales as the field attempts to achieve equilibrium while conserving magnetic helicity. Under suitable conditions, Field and Carroll (2000) showed that astrophysically interesting fields with strength 10^{-10} G 10 kpc scales could be generated during the electroweak phase transition.

4.4 Plasma Processes Capable of Generating Magnetic Fields

4.4.1 Chromodynamic Magnetic Fields?

The QCD regime lasts from the end of reheating until hadron formation, roughly $t_{ns} \sim 10^{-6}$ s after the Big Bang (see Fig. 3). In this regime, matter comprises massive bosons, gluons, quarks and leptons and forms a hot dense chromoplasma or quark–gluon plasma (QGP). At the higher temperatures, that is, not too long after reheating, the QGP is asymptotically free and can be considered collisionless. Since many of the particles in the QGP carry electric charge, under certain conditions, they can generate induced Yang–Mills currents $j^{\mu}_{a}(x) = D_{\mu}F^{\mu\nu}(x)$, with Yang–Mills field $F_{\mu\nu} = A_{\nu,\mu} - A_{\mu,\nu} - ig[A_{\mu}, A_{\nu}]$ expressed through the non-Abelian gauge field $A_{a;\nu}(x)$. The colour index a corresponds to the $N^2 - 1$ colour channels. These currents couple to the electromagnetic gauge field and consequently are accompanied by magnetic fields. Several mechanisms associated with the QCD phase transition were discussed in the previous section. Here we explore whether plasma instabilities in the thermal QGP could possibly lead to appreciable fields. In the context of magnetic field generation in the early universe and cosmology this possibility has not yet been considered; it has, however, been investigated in high-energy physics not working in a comoving system.

The simplest plasma mechanism capable of magnetic field generation is the Weibel (current filamentation)[3] instability first discovered in classical plasma (Weibel 1959). Its free energy is provided by a local pressure anisotropy $A = P_{\parallel}/P_{\perp} - 1 \neq 0$ in the non-magnetic plasma. The subscripts $\parallel, \perp$ refer to the two orthogonal directions $\hat{\parallel}, \hat{\perp}$ of the pressure tensor $\mathsf{P} = P_{\perp}\mathsf{I} + (P_{\parallel} - P_{\perp})\hat{\parallel}\hat{\parallel}$ whose non-diagonal (dissipative) elements are small (Blaizot and Iancu 2002). Pressure anisotropy creates microscopic currents and hence microscopic magnetic fields. Free energy can also be provided by partonic beams passing the QGP. Such beams, when produced by some independent process naturally introduce a preferred direction and may cause additional pressure anisotropy by dissipating their momentum in some (collisionless) way.

Assuming that a cold partonic beam passes the QGP, both analytical theory and numerical simulations (Arnold and Moore 2006a, 2006b; Arnold 2007; Arnold and Moore 2007;

[3]For a discussion of its physics in classical plasmas see Fried (1959).

Arnold and Leang 2007; Rebhan et al. 2008; Romatschke and Rebhan 2006; Schenke et al. 2008; Strickland 2007a, 2007b) prove that the QCD beam-driven Weibel instability excites magnetic fields which subsequently scatter and thermalize the beams by magnetizing the partons. The linear waves, that is, oscillations of the effective quark phase-space momentum distribution $\Phi_{\rm eff}(p)$ as function of the 4-momentum, $p \equiv (p^0, \mathbf{p})$, are solutions of the semi-classical QGP dispersion relation (Pokrovsky and Selikhov 1988; Mrówczyński 1988, 1993) in Fourier 4-space $k = (\omega/c, \mathbf{k})$

$$\det\left[\mathbf{k}^2\delta^{ij} - k^i k^j - \omega^2 \epsilon^{ij}(|\mathbf{k}|)\right] = 0 \tag{26}$$

with ϵ^{ij} the permeability ($v^i = p^i/\sqrt{p^l p_l}$ is the 4-velocity) given as functional of the effective phase space density $\Phi_{\rm eff}(\mathbf{p})$, which does not depend any more on the colour index

$$\epsilon^{ij}(\omega, \mathbf{k}) = \delta^{ij} + \frac{g^2}{2\omega^2}\int \frac{d^3p}{8\pi^3}\frac{v^i[\partial\Phi_{\rm eff}(\mathbf{p})/\partial p^l]}{\omega - \mathbf{k}\cdot\mathbf{v} + i0}\left[(\omega - \mathbf{k}\cdot\mathbf{v})\delta^{lj} + k^l v^j\right]. \tag{27}$$

Instability is found for low frequency ($\omega \approx 0$) non-oscillatory (filamentation) modes with wave vectors, $k_\perp$, perpendicular to the parton-beam 4-velocity, U. The implication is that stationary magnetic fields are generated in this process.

Analytical growth rates of transverse modes, where $\mathrm{Im}\,\omega > 0$, have been obtained for simple Gaussian and other mock equilibrium particle distributions and nuclear physics parameters. All calculations performed refer to non-comoving physical systems. Arnold (2007) has shown that the breakdown of perturbation theory at momenta $p \sim g^2 T$ and the fact that theory becomes non-perturbative at high T implies that it can be treated as if one had a cold plasma, $T = 0$, plus weak coupling. Thus, the semi-classical approach describes long-range properties.[4] In the numerical simulations one takes advantage of this fact, linearises around a stationary homogeneous locally colourless state (Blaizot and Iancu 2002), and considers the evolution of the fluctuation $W^\mu(v, x)$ of the distribution function according to the non-Abelian Vlasov equation and Yang–Mills current density:

$$v_\mu D^\mu W^\nu(\mathbf{v}, x) = -v_\sigma F^{\sigma\nu}(x), \qquad j^\nu(x) = -g^2\int \frac{d^3p}{8\pi^3}\frac{p^\nu}{|\mathbf{p}|}\frac{\partial\Phi_{\rm eff}(\mathbf{p})}{\partial p^\sigma}W^\sigma(\mathbf{v}, x), \tag{28}$$

where the 4-velocity v^ν enters the field equations which close the system and describe the evolution of fields and particles,

$$\left.\begin{aligned} v_\mu D^\mu W^\nu &= -g(\mathbf{E} + \mathbf{v}\times\mathbf{B})\cdot\nabla_{\mathbf{p}}\Phi_{\rm eff} \\ D_\mu F^{\mu\nu} &= -g^2(2\pi)^{-3}\textstyle\int d^3p\, v^\nu (D^\nu)^{-1}(\mathbf{E} + \mathbf{v}\times\mathbf{B})\cdot\nabla_{\mathbf{p}}\Phi_{\rm eff} \end{aligned}\right\}. \tag{29}$$

Instability requires anisotropy to lowest order O(1) in $\mathbf{p}$ of the effective distribution $\Phi_{\rm eff}(\mathbf{p})$ (Arnold and Moore 2006a). The maximum unstable wave vector k_m and growth rate $\gamma_m \equiv +(\mathrm{Im}\,\omega)_m$ of the QCD Weibel mode scale as

$$k_m^2 \sim \gamma_m^2 \sim m_\infty^2 \sim g^2\int_{\mathbf{p}_>} \Phi_{\rm eff}(\mathbf{p})/|\mathbf{p}| \tag{30}$$

[4] The scalar potential A^0 picks up a Debye screening mass m_D and decouples at distances $\gg m_D^{-1} \sim (gT)^{-1}$ leaving the vector potential (transverse chromo-electromagnetic) fields, which is equivalent to classical plasmas where at frequencies $\omega > \omega_p$ above the plasma frequency ω_p any propagating perturbation is purely electromagnetic.

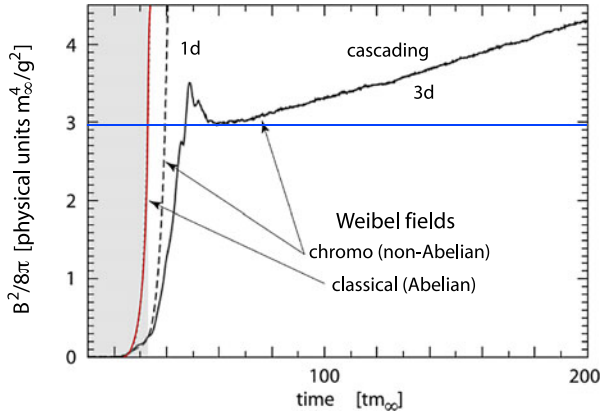

Fig. 4 Numerical simulation results of Weibel fields under Abelian and non-Abelian (QGP) conditions (after Arnold and Moore 2006a). The Abelian and spatially 1d-cases have a long linear phase of exponential growth. The corresponding linear phase in the spatially 3d-case is very short (*shaded region*), followed by a nonlinearly growing phase which reaches maximum field strength and afterward increases weakly and linearly. Closer investigation has shown that this further linear growth is caused by cascading to shorter wavelength (larger k) related to increasing frequencies thereby dispersing the free energy that feeds the nonlinear phase into a broad spectrum of magnetic oscillations. The *blue horizontal line* is the nonlinear saturation level of the low-frequency long-wavelength Weibel magnetic field that persists during the cascade and presumably survives it

where $m_\infty \sim g\sqrt{N_>/p_>}$ is the "effective mass" scale defined by the spatial beam number density $N_>$ of particles with momentum $p_>$ which contribute to the anisotropy, i.e. $N_> \equiv \int_{p_>} \Phi_{\rm eff}(\mathbf{p}) d^3p/8\pi^3$.

Figure 4 plots three simulation results: an Abelian run, a spatially 1d, and a spatially 3d-non-Abelian run. Shown is the magnetic fluctuation energy density $B^2/8\pi$ as function of time (all in proper simulation units). The Abelian and the 1d-non-Abelian cases cover just their linear (exponentially growing) phases. The 3d-non-Abelian case differs from these in several important respects. Its linear phase is very short, shown as the shaded region. It is followed by a longer nonlinear growth phase when the magnetic energy density increases at a slower and time dependent rate until reaching maximum, when it starts decaying. Afterwards it recovers to end up in a further slow but now purely algebraic linear growth.

4.4.1.1 Weibel Saturation Level The nonlinear phase wave-particle interaction terms come progressively into play when the field energy increases. The subsequent slow linear growth phase results from the sudden onset of a (turbulent) cascade from 'long' to short wavelengths and higher frequencies. This cascade has been demonstrated in simulations (Arnold and Moore 2006b; Arnold and Leang 2007). The settings of the simulations are physical not taking into account any general relativistic effects (which should be weak compared to QCD interactions) nor cosmological expansion. The cascade distributes the energy that is fed into the longest unstable scales over a broad range of short scales and higher frequencies $\omega \neq 0$, thereby identifying the nonlinear state of the QGP Weibel instability as short-scale turbulence hosting a mixture of propagating waves. So far it lacks any process (e.g. an inverse cascade) in which the Weibel fields produce large-scale stationary cosmological magnetic fields. In the average the energy density in the Weibel 'long' wavelength domains stays at a constant level

$$\mathcal{E}^{\rm sat}_{\rm Weibel} \lesssim 3m_\infty^4/g^2. \tag{31}$$

For the coupling constant one may use (Bethke 2009) the "world-average value" $g^2 = 4\pi\alpha_s(M_Z^2) \approx 4\pi \times 0.12 = 0.48\pi$, where M_Z is the mass of the Z boson, while for m_∞^2 additional knowledge is required of the effective parton distribution $\Phi_{\rm eff}$, i.e. the state of the undisturbed distribution including the anisotropy.

Unfortunately, the above formula cannot be used directly to estimate the long-wavelength Weibel field saturation value in the early universe. If we accept that the saturation level is robust within few orders of magnitude, then, because $m_\infty^2 \sim \omega_p^2/\sqrt{\theta}$, one has as for an estimate (in physical units)

$$B^{\rm sat} \approx \omega_p^2 \sqrt{2\mu_0\hbar/c^3\theta} \tag{32}$$

where ω_p is the effective chromo-plasma frequency $\omega_p^2 = gT/m_D\lambda_D^2$ which is related to the Debye mass m_D, screening length λ_D, and $\theta \sim \tan^{-1}(A^{-1})$ is a given effective anisotropy angle (Arnold and Leang 2007). The definition of θ holds for both, thermal anisotropies $P_\perp/P_\parallel \equiv T_\perp/T_\parallel$ in the thermal Weibel case, and parton beam anisotropies where $A \propto T^{-1}\int_{\mathbf{p}_>} \Gamma(\mathbf{p})\Phi_{\rm eff}(\mathbf{p})d^3p/8\pi^3$ is the 'equivalent' thermal anisotropy caused by the parton beam of Lorentz factor Γ in QGP of isotropic temperature T.

With these numbers one estimates quite a strong (and thus cosmologically unrealistic) saturation magnetic field

$$B^{\rm sat} \approx 10^{-19}(m_e/M_Z\sqrt{\theta})N_{\rm eff} \sim 2 \times 10^{-25}N_{\rm eff}/\sqrt{\theta}\ {\rm G} \tag{33}$$

a value that depends on the effective parton number density to anisotropy ratio holding for small finite anisotropies. Taking, say, $N_{\rm eff} \sim 10^{10}\ {\rm cm}^{-3}$, it yields a substantial saturated low-frequency QGP seed magnetic field of the order of $B^{\rm sat} \sim 10^{-5}/\sqrt{\theta}\ \mu$G.

Thus, the Weibel mechanism is doubtlessly capable of generating substantially strong magnetic fields during the QGP phase. However, these fields have very short correlation lengths, of the order of the parton skin depth or mean free paths and do probably not contribute to the large-scale field in the cosmological evolution.

4.4.1.2 Thermal Fluctuation Level When the QGP phase lacks any thermal anisotropy thermal fluctuations still provide seed magnetic fields at the thermal chromo-dynamic magnetic fluctuation level far below the magnetic saturation level of the Weibel instability. It results from the thermal fluctuations in the microscopic chromo-plasma currents. For its estimation the unknown effective *isotropic equilibrium* distribution $\Phi_{\rm eff}(\mathbf{p})$ and the complex response function, i.e. the QGP polarisation tensor $\Pi^{\mu\nu}$, are needed whose determination requires solution of the equilibrium chromo-Vlasov equation.

For our purposes, a rough estimate of the thermal level can be obtained from the above simulations taking advantage of the evolution equation of the average magnetic energy density $\langle B^2(t)\rangle$ in the 'zero-frequency' domain. The thermal level is not subject to the Weibel mode instability; however the magnetic energy density measured in the Weibel mode at a certain time t_1 in the linear phase has evolved from the background magnetic thermal fluctuation level $\langle b^2(t=0)\rangle$ at time $t=0$ according to

$$\left\langle B^2(t_1)\right\rangle \simeq \left\langle b^2(t=0)\right\rangle \exp(2\gamma_m t) \tag{34}$$

From the linear phase in Fig. 4 we find for the numerically determined linear chromo-Weibel growth rate that $\gamma_m \approx 0.28/m_\infty$. This value used in the last equation yields an approximate (initial) thermal magnetic energy density level of $\langle b^2\rangle \approx 2.88 \times 10^{-8}m_\infty^4 g^{-2}$, which corresponds to a thermal magnetic fluctuation level independent of the Weibel mode of average

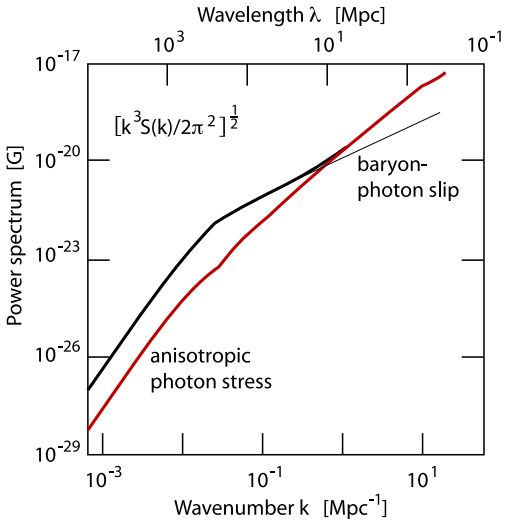

Fig. 5 The spectrum $S(k)$ of magnetic fields in the pre-recombination era generated from cosmological density perturbations (after Ichiki et al. 2006) plotted in units of magnetic field (G) and shown to be composed of contributions from baryon–phonon slip and anisotropic photon stresses. Below roughly $k < 1/\text{Mpc}$ the baryon slip dominates the spectrum while for larger k (shorter wavelength than roughly 10 Mpc) the anisotropic stresses contribute most

amplitude

$$\left\langle b^{\text{th}} \right\rangle \sim 3.4 \times 10^{-29} (N_{\text{eff}}/N) \quad \text{G} \tag{35}$$

during the corresponding QCD phase, depending on the ratio of the effective number density of energetic particles to chromo-plasma density N. This is a low though not unreasonable upper limit on the thermal fluctuation level of stationary ($\omega \approx 0$) QGP collective magnetic seed fields which, however, is probably too low to be of direct astrophysical importance.

4.4.2 Thermal Fluctuations Shortly Before Photon-Matter Decoupling

The previous section dealt with the possible generation of low frequency seed magnetic fields during the QCD phase of the early universe. A more conventional proposal has been elaborated recently (Ichiki et al. 2006, 2006) and is proposed to work during the classical plasma phase before recombination. These authors make the reasonable assumption that during this epoch the coupling between photons and electrons by Compton scattering is much stronger than the coupling between photons and ions. Cautious examination of the particle–photon interaction in a cosmological density fluctuation field indeed shows that pressure anisotropy and currents are induced. The generalised Ohm's law that includes the photon interaction allows for a finite electron current flow because of the differences in the bulk electron and proton velocities caused. This effect produces the desired magnetic fields. However, only the second order density perturbations in the Compton scattering terms lead to fields that survive on a range of spatial scales. The power spectrum $S(k)$ of the fields in the long wavelength range (see Fig. 5) scales as $\sqrt{k^3 S(k)} \propto k$ Here the photon-caused anisotropic stress dominates.

Seed magnetic fields reach values of $B \sim 10^{-18}$ G on scales of $\sim$1 Mpc and $B \sim 10^{-14}$ G on $\sim$10 kpc scales. After decoupling these fields decay adiabatically with expansion of the universe. In a standard cosmology they should today be of strength $B(t_0) \sim 10^{-24}$ G at 1 Mpc and $\sim 10^{-20}$ G at 10 kpc and may have played a role in structure formation after recombination.

These seed fields are surprisingly strong, however. Recently, Fenu et al. (2011) performed numerical simulations taking into account all relevant general relativistic effects. Their esti-

mates based on the WMAP7 parameters suggest that the generation of seed magnetic fields on cosmological scales is mainly related to Compton drag by photons on baryons whereby vorticity is exchanged and magnetic fields are generated still after recombination. The power spectra obtained are $\propto k^4$ for $k \ll k_{eq}$ and $\propto \sqrt{k}$ for $k \gg k_{eq}$ yielding substantially lower comoving fields $B \sim 10^{-29}$ G at 1 Mpc.

5 Magnetic Fields and the Cosmic Microwave Background

The field of cosmology has witnessed a revolution lead, in large part, by detailed measurements of the CMB anisotropy and polarization spectra. Fundamental cosmological parameters such density parameters of baryons, dark matter, and dark energy and the Hubble constant are now known to a precision unimaginable just two decades ago.

If magnetic fields were present at the time of matter-radiation decoupling or soon after, then they would have an effect on the anisotropy and polarization of the CMB (see Subramanian 2006; Durrer 2007 for reviews). First, a very large scale (effectively homogeneous) field would lead to anisotropic expansion and hence to a quadrupole anisotropy in the CMB (see, for example, Thorne 1967). The degree of isotropy of the CMB was used to place a limit of several nG on the strength of such a field redshifted to the current epoch (Barrow et al. 1997). Note, however, that the results of Barrow et al. (1997) assume that magnetic fields are the only source of large-scale anisotropy. Recently, Adamek et al. (2011) showed that neutrinos, which free-stream so long as they are relativistic, generate an anisotropic pressure which can counteract the anisotropic pressure generated by a homogeneous magnetic field. This result depends on the neutrino masses but may damp the effect of very large scale magnetic fields on the CMB.

Primordial magnetogenesis scenarios on the other hand generally lead to tangled fields, plausibly Gaussian random, characterized by say a spectrum $M(k)$. This spectrum is normalized by giving the field strength B_0, at some fiducial scale, and as measured at the present epoch, assuming it decreases with expansion as $B = B_0/a^2(t)$. Since magnetic and radiation energy densities both scale with expansion as $1/a^4$, we can characterize the magnetic field effect by the ratio $B_0^2/(8\pi\rho_{\gamma 0}) \sim 10^{-7} B_{-9}^2$ where $\rho_{\gamma 0}$ is the present day energy density in radiation, and $B_{-9} = B_0/(10^{-9}$ G). Magnetic stresses are therefore small compared to the radiation pressure for nano Gauss fields.

Nevertheless, the scalar, vector and tensor parts of the perturbed stress tensor associated with primordial magnetic fields lead to corresponding metric perturbations, including gravitational waves. Further the compressible part of the Lorentz force leads to compressible (scalar) fluid velocity and associated density perturbations, while its vortical part leads to vortical (vector) fluid velocity perturbation. These magnetically induced metric and velocity perturbations lead to both large and small angular scale anisotropies in the CMB temperature and polarization.

The scalar contribution has been the most subtle to calculate, and has only begun to be understood by several groups (Giovannini and Kunze 2008; Yamazaki et al. 2008; Finelli et al. 2008; Shaw and Lewis 2010). The anisotropic stress associated with the magnetic field leads in particular to the possibility of two types of scalar modes, a potentially dominant mode which arises before neutrino decoupling sourced by the magnetic anisotropic stress. And a compensated mode which remains after the growing neutrino anisotropic stress has compensated the magnetic anisotropic stress (cf. Shaw and Lewis 2010; Bonvin and Caprini 2010 for detailed discussion). The magnetically induced compressible fluid perturbations, also changes to the acoustic peak structure of the angular anisotropy power spectrum (see,

for example, Adams et al. 1996). However, for nano Gauss fields, the CMB anisotropies due to the magnetized scalar mode are grossly subdominant to the anisotropies generated by scalar perturbations of the inflaton.

Potentially more important is the contribution of the Alfvén mode driven by the rotational component of the Lorentz force (Subramanian and Barrow 1998; Mack et al. 2002; Subramanian et al. 2003; Lewis 2004). Unlike the compressional mode, which gets strongly damped below the Silk scale, L_S due to radiative viscosity (Silk 1968), the Alfvén mode behaves like an over damped oscillator. This is basically because the phase velocity of oscillations, in this case the Alfvén velocity, is $V_A \sim 3.8 \times 10^{-4} c B_{-9}$ much smaller than the relativistic sound speed $c/\sqrt{3}$. Note that for an over damped oscillator there is one normal mode which is strongly damped and another where the velocity starts from zero and freezes at the terminal velocity till the damping becomes weak at a latter epoch. The net result is that the Alfvén mode survives Silk damping down to much smaller scales; $L_A \sim (V_A/c) L_S \ll L_S$, the canonical Silk damping scale (Jedamzik et al. 1998; Subramanian and Barrow 1998). The resulting baryon velocity leads to a CMB temperature anisotropy, $\Delta T \sim 5 \mu K (B_{-9}/3)^2$ for a scale invariant spectrum, peaked below the Silk damping scale (angular wavenumbers $l > 10^3$). This rough estimate has also been borne out by the detailed calculations of Lewis (2004).

The magnetic anisotropic stress also induces tensor perturbations, resulting in a comparable CMB temperature anisotropy, but now peaked on large angular scales of a degree or more (Durrer et al. 2000). Both the vector and tensor perturbations lead to ten times smaller B-type polarization anisotropy, at respectively small and large angular scales (Seshadri and Subramanian 2001; Subramanian et al. 2003; Mack et al. 2002; Lewis 2004). Note that inflationary generated scalar perturbations only produce the E-type mode. The small angular scale vector contribution in particular can potentially help to isolate the magnetically induced signals (Subramanian et al. 2003).

A crucial difference between the magnetically induced CMB anisotropy signals compared to those induced by inflationary scalar and tensor perturbations, concerns the statistics associated with the signals. Primordial magnetic fields lead to non-Gaussian statistics of the CMB anisotropies even at the lowest order, as magnetic stresses and the temperature anisotropy they induce depend quadratically on the magnetic field. In contrast, CMB non-Gaussianity due to inflationary scalar perturbations arises only as a higher order effect. A computation of the non-Gaussianity of the magnetically induced signal has begun (Seshadri and Subramanian 2009; Caprini et al. 2009; Cai et al. 2010), based on earlier calculations of non-Gaussianity in the magnetic stress energy (Brown and Crittenden 2005). This new direction of research promises to lead to tighter constraints or a detection of strong enough primordial magnetic fields.

A primordial magnetic field leads to a number of other effects on the CMB which can probe its existence: Such a field in the inter galactic medium can cause Faraday rotation of the polarized component of the CMB, leading to the generation of new B-type signals from the inflationary E-mode signal (Kosowsky and Loeb 1996). Any large-scale helical component of the field leads to a parity violation effect, inducing non-zero T-B and E-B cross-correlations (Kahniashvili and Ratra 2005); such cross-correlations between signals of even and odd parity are necessarily zero in standard inflationary models. The damping of primordial fields in the pre-recombination era can lead to spectral distortions of the CMB (Jedamzik et al. 2000), while their damping in the post-recombination era can change the ionization and thermal history of the universe and hence the electron scattering optical depth as a function of redshift (see Sethi and Subramanian 2005; Tashiro and Sugiyama 2006a; Schleicher et al. 2008, and Sect. 5.3). Future CMB probes like PLANCK can potentially

detect the modified CMB anisotropy signal from such partial re-ionization. In summary primordial magnetic fields of a few nG lead to a rich variety of effects on the CMB and thus are potentially detectable via observation of CMB anisotropies.

6 Implications of Strong Primordial Fields in the Post-recombination Universe

If strong magnetic fields have been produced during phase-transitions in the early universe, and if these fields had some non-zero helicity, they may have remained strong until recombination and beyond (Christensson et al. 2001; Banerjee and Jedamzik 2004). They could then affect the thermal and chemical evolution during the dark ages of the Universe, the formation of the first stars, and the epoch of reionization.

6.1 Implications During the Dark Ages

At high redshift $z > 40$, the universe is close to homogeneous, and the evolution of the temperature, T, is governed by the competition of adiabatic cooling, Compton scattering with the CMB and, in the presence of strong magnetic fields, ambipolar diffusion. It is thus given as

$$\frac{dT}{dz} = \frac{8\sigma_T a_R T_{\rm rad}^4}{3H(z)(1+z)m_e c}\frac{x_e(T-T_{\rm rad})}{1+f_{\rm He}+x_e} + \frac{2T}{1+z} - \frac{2(L_{\rm AD}-L_{\rm cool})}{3nk_B H(z)(1+z)}, \tag{36}$$

where $L_{\rm AD}$ is the heating function due to ambipolar diffusion (AD), $L_{\rm cool}$ the cooling function (Anninos et al. 1997), σ_T the Thomson scattering cross section, a_R the Stefan–Boltzmann radiation constant, m_e the electron mass, c the speed of light, k_B Boltzmann's constant, n the total number density, $x_e = n_{\rm e}/n_H$ the electron fraction per hydrogen atom, $T_{\rm rad}$ the CMB temperature, $H(z)$ is the Hubble factor and $f_{\rm He}$ is the number ratio of He and H nuclei.

AD occurs due to the friction between ionized and neutral species, as only the former are directly coupled to the magnetic field. Primordial gas consists of several neutral and ionized species, and for an appropriate description of this process, we thus adopt the multi-fluid approach of Pinto et al. (2008), defining the AD heating rate as

$$L_{\rm AD} = \frac{\eta_{\rm AD}}{4\pi}\left|(\nabla\times\mathbf{B})\times\mathbf{B}/B\right|^2, \tag{37}$$

where $\eta_{\rm AD}$ is given as

$$\eta_{\rm AD}^{-1} = \sum_n \eta_{{\rm AD},n}^{-1}. \tag{38}$$

In this expression, the sum includes all neutral species n, and $\eta_{{\rm AD},n}$ denotes the AD resistivity of the neutral species n. We note that the AD resistivities themselves are a function of magnetic field strength, temperature and chemical composition.

In the primordial IGM, the dominant contributions to the total resistivity are the resistivities of atomic hydrogen and helium due to collisions with protons. These are calculated based on the momentum transfer coefficients of Pinto and Galli (2008). As the power spectrum of the magnetic field is unknown, we estimate the expression in (37) based on the coherence length L_B, given as the characteristic scale for Alfvén damping (Jedamzik et al. 1998;

Subramanian 1998; Seshadri and Subramanian 2001). Contributions from decaying MHD turbulence may also be considered, but are negligible compared to the AD heating (Sethi and Subramanian 2005).

The additional heat input provided by AD affects the evolution of the ionized fraction of hydrogen, $x_{\rm p}$, which is given as

$$\frac{dx_{\rm p}}{dz} = \frac{[x_e x_p n_H \alpha_H - \beta_H (1-x_p) e^{-h_p \nu_{H,2s}/kT}]}{H(z)(1+z)[1+K_H(\Lambda_H+\beta_H) n_H (1-x_p)]} \times \left[1 + K_H \Lambda_H n_H (1-x_p)\right] - \frac{k_{\rm ion} n_H x_p}{H(z)(1+z)}. \tag{39}$$

Here, n_H is the number density of hydrogen atoms and ions, h_p Planck's constant, $k_{\rm ion}$ is the collisional ionization rate coefficient (Abel et al. 1997). Further details of notation, as well as the parametrized case B recombination coefficient for atomic hydrogen α_H, are given by Seager et al. (1999). The chemical evolution of the primordial gas is solved with a system of rate equations for the chemical species H^-, H_2^+, H_2, HeH^+, D, D^+, D^-, $HD^+$and HD based on the primordial rate coefficients tabulated by Schleicher et al. (2008). For the mutual neutralization rate of H^- and H^+, we use the more recent result of Stenrup et al. (2009). The evolution of the magnetic energy density $E_B = B^2/8\pi$ is given as

$$\frac{dE_B}{dt} = \frac{4}{3}\frac{\partial \rho}{\partial t}\frac{E_B}{\rho} - L_{\rm AD}. \tag{40}$$

The first term describes the evolution of the magnetic field in a homogeneous universe in the absence of specific magnetic energy generation or dissipation mechanisms. The second term accounts for corrections due to energy dissipation via AD.

The dynamical implications of magnetic fields can be assessed from the magnetic Jeans mass, the critical mass scale for gravitational forces to overcome magnetic pressure. In the cosmological context, the magnetic Jeans mass is given as (Subramanian 1998; Sethi and Subramanian 2005)

$$M_J^B \sim 10^{10} M_\odot \left(\frac{B_0}{3\ {\rm nG}}\right)^3. \tag{41}$$

We note that this equation is derived in the cosmological context and is only valid on cosmological scales. A more general expression for the magnetic Jeans length is given below.

Due to ambipolar diffusion, strong magnetic fields also affect the gas temperature and thus the thermal Jeans mass, i.e. the critical mass scale required to overcome gas pressure. It is defined as

$$M_J = \left(\frac{4\pi\rho}{3}\right)^{-1/2} \left(\frac{5k_B T}{2\mu G m_P}\right)^{3/2} \tag{42}$$

with Boltzmann's constant k_B, the mean molecular weight μ and the proton mass m_p.

To describe virialization in the first minihalos, we employ the spherical collapse model of Peebles (1993) for pressureless dark matter until an overdensity of ∼200 is reached. Equating cosmic time with the timescale from the spherical collapse model allows one to calculate the overdensity ρ/ρ_b as a function of time or redshift. In this model, we further assume that the formation of the protocloud will reduce the coherence length of the magnetic field to the size of the cloud.

The evolution of the magnetic field strength, the IGM temperature and the chemical abundances of different species have been calculated by Schleicher et al. (2009b) using an

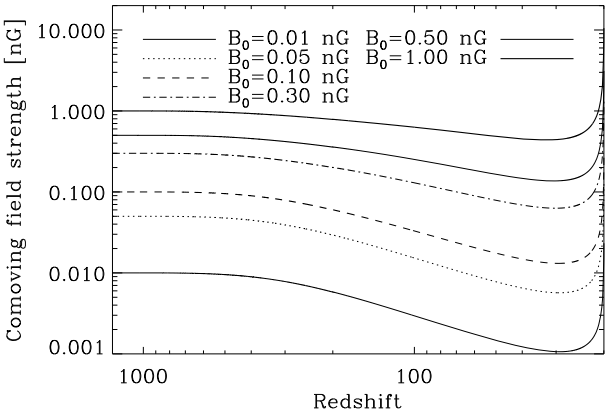

Fig. 6 The evolution of the comoving magnetic field strength due to AD as a function of redshift for different initial comoving field strengths, from the homogeneous medium at $z = 1300$ to virialization at $z = 20$

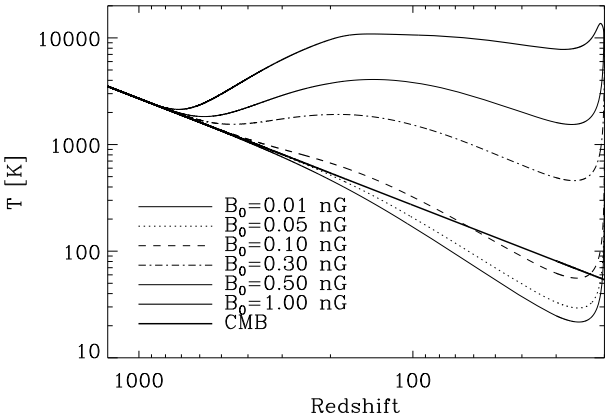

Fig. 7 The gas temperature evolution in the IGM as a function of redshift for different comoving field strengths, from the homogeneous medium at $z = 1300$ to virialization at $z = 20$. For the case with $B_0 = 0.01$ nG, we find no difference in the thermal evolution compared to the zero-field case

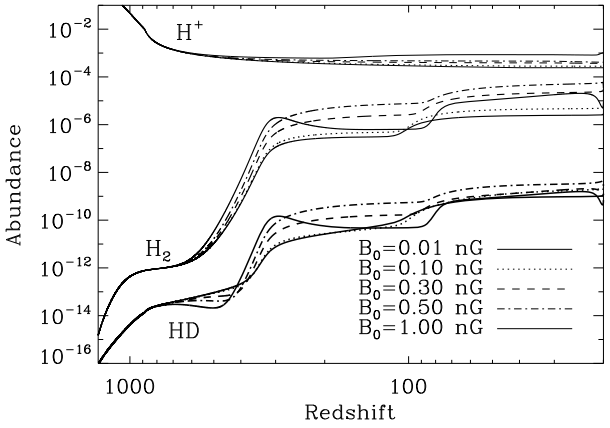

Fig. 8 The evolution of ionization degree, H_2 and HD abundances as a function of redshift for different comoving field strengths, from the homogeneous medium at $z = 1300$ to virialization at $z = 20$. For the case with $B_0 = 0.01$ nG, we find no difference in the chemical evolution compared to the zero-field case

extension of the recombination code RECFAST (Seager et al. 1999). The results are shown in Figs. 6, 7 and 8. As shown in Fig. 6, ambipolar diffusion primarily affects magnetic fields with initial comoving field strengths of 0.2 nG or less. For stronger fields, the dissipation of only a small fraction of their energy increases the temperature and the ionization fraction

of the IGM to such an extent that AD becomes less effective. For comoving field strengths up to $\sim$0.1 nG, the additional heat from ambipolar diffusion is rather modest and the gas in the IGM cools below the CMB temperature due to adiabatic expansion. However, it can increase significantly for stronger fields and reaches $\sim 10^4$ K for a comoving field strength of 1 nG, where Lyman α cooling and collisional ionization become efficient and prevent a further increase in temperature. The increased temperature enhances the ionization fraction and leads to larger molecule abundances at the onset of star formation.

6.2 Implications for the Formation of the First Stars

We now explore in more detail the consequences of magnetic fields for the formation of the first stars, during the protostellar collapse phase. For this purpose, a model describing the chemical and thermal evolution during free-fall collapse was developed by Glover and Savin (2009) and extended by Schleicher et al. (2009b) for the effects of magnetic fields. Particularly important with respect to this application is the fact that it correctly models the evolution of the ionization degree and the transition at densities of $\sim 10^8$ cm^{-3} where Li^+ becomes the main charge carrier. Based on the Larson–Penston type self-similar solution (Larson 1969; Penston 1969; Yahil 1983), we evaluate how the collapse timescale is affected by the thermodynamics of the gas.

During protostellar collapse, magnetic fields are typically found to scale as a power-law with density ρ. Assuming ideal MHD with flux freezing and spherical symmetry, one expects a scaling with $\rho^{2/3}$ in the case of weak fields. Deviations from spherical symmetry such as expected for dynamically important fields give rise to shallower scalings, e.g. $B \propto \rho^{0.6}$ (Banerjee et al. 2004; Banerjee and Pudritz 2006), $B \propto \rho^{1/2}$ (Hennebelle and Fromang 2008; Hennebelle and Teyssier 2008). Based on numerical simulations of Machida et al. (2006), we find an empirical power-law relation $B \propto \rho^{\alpha}$ where

$$\alpha = 0.57 \left(\frac{M_J}{M_J^B} \right)^{0.0116} . \tag{43}$$

In a collapsing cloud, the more general expression for the magnetic Jeans mass,

$$M_J^B = \frac{\Phi}{2\pi\sqrt{G}}, \tag{44}$$

is adopted. In this prescription, $\Phi = \pi r^2 B$ denotes the magnetic flux, G the gravitational constant, r an appropriate length scale. The calculation of the magnetic Jeans mass thus requires an assumption regarding the size of the dense region. Numerical hydrodynamics simulations show that they are usually comparable to the thermal Jeans length (Abel et al. 2002; Bromm and Larson 2004). This is also suggested by analytical models for gravitational collapse (Larson 1969; Penston 1969; Yahil 1983).To account for magnetic energy dissipation via AD, we calculate the AD heating rate from (37) and correct the magnetic field strength accordingly. We note that due to the large range of densities during protostellar collapse, additional processes need to be taken into account to calculate the AD resistivity correctly. In particular, at a density of $\sim 10^9$ cm^{-3}, the three-body H_2 formation rates start to increase the H_2 abundance significantly, such that the gas is fully molecular at densities of $\sim 10^{11}$ cm^{-3}. As a further complication, the proton abundance drops considerably at densities of $\sim 10^8$ cm^{-3}, such that Li^+ becomes the main charge carrier (Maki and Hajime 2004; Glover and Savin 2009). These effects are incorporated in our multi-fluid approach.

Table 1 The physical field strength B at beginning of collapse as a function of the comoving field strength B_0 used to initialize the IGM calculation at $z = 1300$

B_0 [nG]	B [nG]
1	4.8×10^3
0.3	6.3×10^2
0.1	1.3×10^2
0.01	1.0×10^1

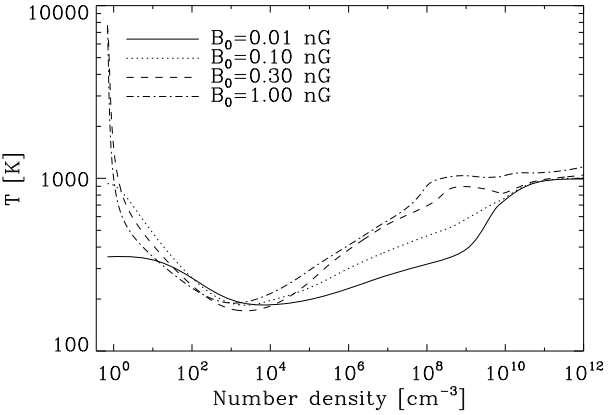

Fig. 9 The gas temperature as a function of density for different comoving field strengths. For $B_0 = 0.01$ nG, the thermal evolution corresponds to the zero-field case

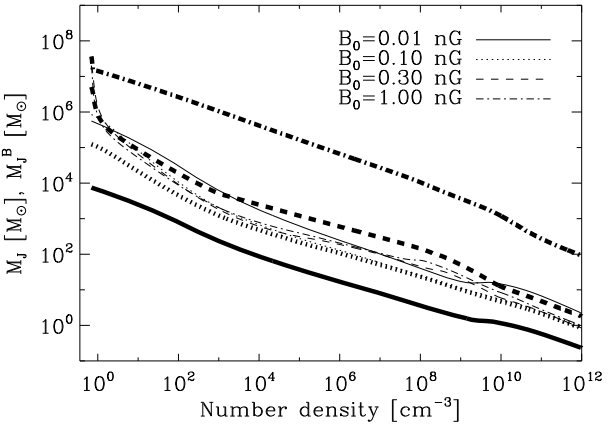

Fig. 10 Thermal (*thin lines*) and magnetic (*thick lines*) Jeans mass as a function of density for different comoving field strengths. For $B_0 = 0.01$ nG, the thermal evolution and thus the thermal Jeans mass corresponds to the zero-field case

As an initial condition for these model calculations, we use the physical field strength and the chemical abundances obtained from the spherical collapse model in Sect. 6.1. The relation between co-moving and physical field strength at the beginning of this calculation is thus given in Table 1.

Figure 9 shows the calculated temperature evolution as a function of density for different comoving field strengths. For comoving fields of 0.01 nG or less, there is virtually no difference in the temperature evolution from the zero-field case. For comoving fields of ∼0.1 nG, cooling wins over the additional heat input in the early phase of collapse, and the temperature decreases slightly below the zero-field value at densities of 10^3 cm^{-3}. At higher densities, the additional heat input dominates over cooling and the temperature steadily increases. At

densities of $\sim 10^9$ cm^{-3}, the abundance of protons drops considerably and increases the AD resistivity defined in (38) and the heating rate until Li^+ becomes the main charge carrier. In particular for comoving fields larger than ~ 0.1 nG, this transition is reflected by a small bump in the temperature evolution due to the increased heating rate in this density range.

Apart from the transition where Li^+ becomes the dominant charge carrier, the magnetic field strength usually increases more rapidly than $\rho^{0.5}$, and weak fields increase more rapidly than strong fields. This is what one naively expects from (43), and it is not significantly affected by magnetic energy dissipation. Another important point is that comoving fields of only 10^{-5} nG are amplified to values of ~ 1 nG at a density of 10^3 cm^{-3}. Such fields are required to drive protostellar outflows that can magnetize the IGM (Machida et al. 2006).

Figure 10 shows the evolution of the thermal and magnetic Jeans mass during collapse. The thermal Jeans masses are quite different initially, but as the temperatures reach the same order of magnitude during collapse, the same holds for the thermal Jeans mass. The thermal Jeans mass in this late phase has only a weak dependence on the field strength. As expected, the magnetic Jeans masses are much more sensitive to the magnetic field strength, and initially differ by about two orders of magnitude for one order of magnitude difference in the field strength. For comoving fields of ~ 1 nG, the magnetic Jeans mass dominates over the thermal one and thus determines the mass scale of the protocloud. For ~ 0.3 nG, both masses are roughly comparable, while for weaker fields the thermal Jeans mass dominates. The magnetic Jeans mass shows features both due to magnetic energy dissipation, but also due to a change in the thermal Jeans mass, which sets the typical length scale and thus the magnetic flux in the case that $M_J > M_J^B$.

The uncertainties in these models have been explored further by Schleicher et al. (2009b), and an independent calculation including stronger magnetic fields has been provided by Sethi et al. (2010). We also note that the consequences of initially weak magnetic fields for primordial star formation are explored in more detail in the next chapter.

6.3 Implications for Reionization

Strong magnetic fields may influence the epoch of reionization in various ways. As discussed above, they may affect the formation of the first stars and change their mass scale, and thus their feedback effects concerning cosmic reionization and metal enrichment. They may further give rise to fluctuations in the large-scale density field and potentially enhance high-redshift structure formation (Kim et al. 1996; Sethi and Subramanian 2005; Tashiro and Sugiyama 2006a). On the other hand, the increased thermal and magnetic pressure may indeed suppress star formation in small halos and thus delay reionization (Schleicher et al. 2008; Rodrigues et al. 2010). In both cases, unique signatures of the magnetic field may become imprinted in the 21 cm signature of reionization, which may help to constrain or detect such magnetic fields with LOFAR,[5] EDGES[6] or SKA[7] (Tashiro and Sugiyama 2006b; Schleicher et al. 2009a). Upcoming observations of these facilities may thus provide a unique opportunity to probe high-redshift magnetic fields in more detail.

[5]LOFAR homepage: http://www.lofar.org/.

[6]EDGES homepage: http://www.haystack.mit.edu/ast/arrays/Edges/.

[7]SKA homepage: http://www.skatelescope.org/.

7 Seed Fields in the Post-recombination Universe

We have seen that magnetic fields arise naturally during inflation and during phase transitions after inflation but before recombination. However, the effective field strength on galactic scales may be exceedingly small. Indeed, the seed fields for the galactic dynamo may well arise from astrophysical processes rather than exotic early-Universe ones. In this section, we review three processes that can generate magnetic field in the post-recombination Universe.

7.1 Biermann Battery

In the hierarchical clustering scenario, proto-galaxies acquire angular momentum from tidal torques produced by neighboring systems (Hoyle 1949; Peebles 1969; White 1984). However, these purely gravitational forces cannot generate vorticity (the gravitational force can be written as the gradient of a potential whose curl is identically zero) and therefore the existence of vorticity must arise from gasdynamical processes such as those that occur in shocks. More specifically, vorticity is generated whenever one has crossed pressure and density gradients. In an ionized plasma, this situation drives currents which, in turn, generate magnetic field. This mechanism, known as the Biermann battery and originally studied in the context of stars (Biermann 1950) was considered in the cosmological context by Pudritz and Silk (1989), Kulsrud et al. (1997), Davies and Widrow (2000), and Xu et al. (2008).

In magnetohydrodynamics, the time dependence of the magnetic field can be written as:

$$\frac{\partial \mathbf{B}}{\partial t} = \nabla \times (\mathbf{v} \times \mathbf{B}) + \frac{c^2}{4\pi\sigma}\nabla^2 \mathbf{B}, \tag{45}$$

where σ is the conductivity, which is assumed to be constant in space. The Biermann effect leads to an additional source term for $\partial \mathbf{B}/\partial t$ of the form

$$\frac{m_e c}{e}\frac{\nabla p_e \times \nabla \rho_e}{\rho_e^2}, \tag{46}$$

where p_e and ρ_e are the electron pressure and density.

The equation for the vorticity, ω, has a similar source term:

$$\frac{\partial \omega}{\partial t} = \nabla \times (\mathbf{v} \times \omega) + \frac{\nabla p \times \nabla \rho}{\rho^2}, \tag{47}$$

where, here, p and ρ refer to the whole fluid. The implication is that when vorticity is generated, so it magnetic field. A simple order of magnitude estimate yields

$$B_{\text{Biermann}} \simeq \frac{m_p c}{e}\omega \simeq 3 \times 10^{-21} \left(\frac{\omega}{\text{km s}^{-1}\,\text{kpc}^{-1}}\right) \text{Gauss}. \tag{48}$$

We note that the vorticity in the solar neighborhood is of order 30 $\text{km s}^{-1}\,\text{kpc}^{-1}$ so for galactic-scale fields, we may expect seed fields of order 10^{-19} G from the Biermann mechanism.

The Biermann effect is expected to arise in a wide range of astrophysical settings. Lazarian (1992) showed that a Biermann-type effect operates in the interstellar medium, which is, in general, non-uniform, multiphase, and clumpy. Of particular interest is the epoch of reionization, which occurs at a redshift $z \sim 10$. During this epoch, photons from descrete sources

such as QSOs and first-generation stars, reionize the intergalactic medium. Reionization begins when ionization fronts propagate away from these sources. Since the pressure and density (or temperature) gradients in these fronts are, in general, misaligned, one can expect the Biermann mechanism to operate and generate seed magnetic fields (Subramanian et al. 1994; Gnedin et al. 2000).

Any force that acts differently on electrons and protons will drive currents and hence generate magnetic fields. The Biermann battery is but one example. Radiation pressure, which will also be important during reionization, acts more strongly on electrons than protons and will therefore drive electric currents (Langer et al. 2003; Ando et al. 2010).

7.2 First-Generation Stars

The first generation of stars provides another potential source of seed fields for the galactic dynamo. Even if stars are born without magnetic fields, a Biermann battery will generate weak fields which can then be rapidly amplified by a stellar dynamo. If the star subsequently explodes or loses a significant amount of mass through stellar winds, the fields will find their way into the interstellar medium and spread throughout the (proto) galaxy. Simple estimates by Syrovatskii (1970) illustrate the viability of the mechanism. There have been some 10^8 supernovae over the lifetime of the galaxy, each of which spreads material through a $(10\ \mathrm{pc})^3$ volume. Using values for the field strength typical of the Crab nebula, one therefore expects the galaxy to be filled by 10 pc regions with field strengths $\sim$3 μG. Assuming the same $L^{-\beta}$ scaling discussed above, one finds a field strength of 10^{-13} G on 10 kpc scales (assuming $\beta = 5/2$ as in Durrer and Caprini 2003), a value significantly larger than the ones obtained by more exotic early Universe mechanisms.

The strong amplification of seed magnetic fields during primordial star formation has been suggested in a number of works. Analytical estimates by Pudritz and Silk (1989), Tan and Blackman (2004), and Silk and Langer (2006) suggest that large-scale dynamos as well as the magneto-rotational instability could significantly amplify weak magnetic seed fields until saturation. Even before, during the protostellar collapse phase, the small-scale dynamo leads to an exponential growth of the magnetic fields, as found in both semi-analytic and numerical studies (Schleicher 2010; Sur et al. 2010).

7.3 Active Galactic Nuclei

Strong magnetic fields almost certainly arise in active galactic nucleii (AGN). These fields will find their way into the intergalactic medium via jets thereby providing a potential source of magnetic field for normal galaxies (Hoyle 1969; Rees 1987, 1994; Daly and Loeb 1990). The potential field strengths due to this mechanism may be estimated as follows: The rotational energy associated with the central compact (mass M) object which powers the AGN can be parametrized as fMc^2 where $f < 1$. If we assume equipartition between rotational and magnetic energy within a central volume V_c, we find

$$B_c = \left(\frac{8\pi f M c^2}{V_c} \right)^{1/2}. \tag{49}$$

If this field then expands adiabatically to fill a "galactic" volume V_g one finds $B_g = B_c (V_c / V_g)^{2/3}$. Hoyle (1969) considered values $M = 10^9\, M_\odot$, $f = 0.1$, $V_g \simeq (100\ \mathrm{kpc})^3$ and found $B_c \simeq 10^9$ G and $B_g \simeq 10^{-5}$ G.

8 Conclusions

The origin of the seed magnetic fields necessary to prime the galactic dynamo remains a mystery and one that has become more, rather than less, perplexing over the years as observations have pushed the epoch of microgauss galactic fields back to a time when the Universe was a third its present age. Numerous authors have explored the possible that the galactic fields observed today and at intermediate redshift have their origin in the very early Universe.

The impetus for the study of early Universe magnetic fields came from the successful marriage of ideas from particle physics and cosmology that occurred during the latter half of the last century. It is a remarkable prediction of modern cosmology that the particles and fields of the present-day Universe emerged during phase transitions a fraction of a second after the Big Bang. The electromagnetic and weak interactions became distinct during the electroweak phase transitions at $t \simeq 10^{-12}$ s while baryons replaced the quark–gluon plasma at $t \simeq 10^{-6}$ s. Perhaps more fantastical is the notion that galaxies, clusters, and superclusters arose from quantum-produced density perturbations that originated during inflation at even earlier times. This idea is supported by strong circumstantial from the CMB anisotropy spectrum, so much so, that it is now part of the standard lore of modern cosmology.

Both inflation and early Universe phase transitions have many of the ingredients necessary for the creation of magnetic fields. If our understanding of inflation-produced density perturbations is correct, the similar quantum fluctuations in the electromagnetic field will lead to fields on the scales of galaxies and beyond. As well, electromagnetic currents, and hence fields, will almost certainly be driven during both the electroweak and quark–hadron phase transitions.

Early Universe schemes for magnetic field generation, however, face serious challenges. In the standard electromagnetic theory, and in a flat or closed FLRW cosmology, inflation-produced fields at diluted by the expansion to utterly negligible levels. One may address this issue by considering fields in an open Universe and "just-so" inflation scenario, that is, a scenario with just enough e-folds of inflation to solve the flatness problem. Alternatively, one may incorporate additional couplings of the field to gravity into the theory though many terms lead to unwanted consequences which render the theory unphysical. Observations and advances in theoretical physics may settle the issue. For example, if future determinations find that the Universe has a slight negative curvature (density parameter for matter and dark energy slightly less than one), it would give some credence to the idea of superadiabatic field amplification in an open Universe. On the other hand, string theory may point us to couplings between gravity and electromagnetism that naturally generate fields during inflation.

The main difficulty with fields generated from phase transitions after inflation arises from the small Hubble scale in the very early Universe. Strong fields are almost certainly produced by one of a number of mechanism. But the coherence length is so small, the effective field strength on galactic scales is likely to be well-below the level of interest for astrophysics. An inverse cascade may help; if the field has a net helicity, the magnetic field energy will be efficiently transferred from small to large scales. But even if fields are uninteresting for the galactic dynamo, they may have an effect on processes in the post-recombination Universe such as reionization and the formation of the first generation of stars.

Where, if not the early Universe, did the seed fields for the galactic dynamo arise? Astrophysics provides a number of promising alternatives. Galactic disks have angular momentum *and* vorticity. While the former is generated by the gravitational interaction between neighboring protogalaxies, the latter comes form gasdynamical effects which necessarily generate

magnetic fields via the Biermann battery. As well, magnetic fields, rapidly created and amplified inside some early generation of stars or in active galactic nucleii, can be dispersed throughout the intergalactic medium.

Acknowledgements DR is supported by National Research Foundation of Korea through grant 2007-0093860. LMW is supported by a Discovery Grant from the Natural Sciences and Engineering Research Council of Canada.

References

T. Abel, P. Anninos, Y. Zhang, M.L. Norman, New Astron. **2**, 181 (1997)
T. Abel, G.L. Bryan, M.L. Norman, Science **295**, 93 (2002)
J. Adamek, R. Durrer, F. Elisa, M. Vonlanthen, J. Cosmol. Astropart. Phys. **6**, 17 (2011)
J. Adams, U.H. Danielsson, D. Grasso, H. Rubinstein, Phys. Lett. B **388**, 253 (1996)
S. Ando, A. Kusenko, arXiv:1005.1924 (2010)
M. Ando, K. Doi, H. Susa, Astrophys. J. **716**, 1566 (2010)
P. Anninos, Y. Zhang, T. Abel, M.L. Norman, New Astron. **2**, 209 (1997)
P. Arnold, G.D. Moore, Phys. Rev. D **73**, 025006 (2006a)
P. Arnold, G.D. Moore, Phys. Rev. D **73**, 025013 (2006b)
P. Arnold, Int. J. Mod. Phys. E **16**, 2555–2594 (2007)
P. Arnold, G.D. Moore, Phys. Rev. D **76**, 045009 (2007)
P. Arnold, P.S. Leang, Phys. Rev. D **76**, 065012 (2007)
R.M. Athreya, V.K. Kapahi, P.J. McCarthy, W. van Breugel, Astron. Astrophys. **329**, 809 (1998)
R. Banerjee, K. Jedamzik, Phys. Rev. D **70**, 123003 (2004)
R. Banerjee, R.E. Pudritz, Astrophys. J. **641**, 949 (2006)
R. Banerjee, R.E. Pudritz, L. Holmes, Mon. Not. R. Astron. Soc. **355**, 248 (2004)
J.D. Barrow, C.G. Tsagas, Phys. Rev. D **77**, 107302 (2008)
J.D. Barrow, C.G. Tsagas, Mon. Not. R. Astron. Soc. **414**, 312 (2011)
J.D. Barrow, P.G. Ferreira, J. Silk, Phys. Rev. Lett. **78**, 3610–3613 (1997)
A. Brandenburg, Phys. Rev. D **54**, 1291 (1996)
I. Brown, R. Crittenden, Phys. Rev. D **72**, 063002 (2005)
M.L. Bernet, F. Miniati, S. J Lilly, P.P. Kronber, M. Dessauges-Zavadsky, Nature **454**, 302 (2008)
S. Bethke, Eur. Phys. J. C **64**, 689–703 (2009)
L. Biermann, Z. Naturforsch. A **5**, 65 (1950)
J.-P. Blaizot, E. Iancu, Phys. Rep. **359**, 355 (2002)
C. Bonvin, C. Caprini, J. Cosmol. Astropart. Phys. **5**, 022 (2010)
V. Bromm, R.B. Larson, Annu. Rev. Astron. Astrophys. **42**, 79 (2004)
R.-G. Cai, B. Hu, H.-B. Zhang, J. Cosmol. Astropart. Phys. **8**, 025 (2010)
C. Caprini, F. Finelli, D. Paoletti, A. Riotto, J. Cosmol. Astropart. Phys. **6**, 021 (2009)
C.L. Carilli, K.M. Menten, Annu. Rev. Astron. Astrophys. **40**, 319 (2002)
B. Cheng, A.V. Olinto, Phys. Rev. D **50**, 2421 (1994)
M. Christensson, M. Hindmarsh, A. Brandenburg, Phys. Rev. E **64**, 056405 (2001)
J.M. Cornwall, Phys. Rev. D **56**, 6146 (1997)
R.A. Daly, A. Loeb, Astrophys. J. **355**, 416 (1990)
G. Davies, L.M. Widrow, Astrophys. J. **540**, 755 (2000)
V. Demozzi, V. Mukhanov, H. Rubinstein, J. Cosmol. Astropart. Phys. **8**, 25 (2009)
C.D. Dermer et al., Astrophys. J. **733L**, 21 (2011)
R. Durrer, L. Hollenstein, R.K. Jain, J. Cosmol. Astropart. Phys. **3**, 37 (2011)
R. Durrer, New Astron. Rev. **51**, 275 (2007)
R. Durrer, C. Caprini, J. Cosmol. Astropart. Phys. **11**, 10 (2003)
R. Durrer, P.G. Ferreira, T. Kahniashvili, Phys. Rev. D **61**, 043001 (2000)
E. Fenu, C. Pitrou, R. Maartens, Mon. Not. R. Astron. Soc. **414**, 580 (2011). doi:10.1111/j.1365-2966.2011.18554.x
G.B. Field, S.M. Carroll, Phys. Rev. D **62**, 103008 (2000)
F. Finelli, F. Paci, D. Paoletti, Phys. Rev. D **78**, 023510 (2008)
B.D. Fried, Phys. Fluids **2**, 337 (1959)
U. Frisch et al., J. Fluid Mech. **68**, 769 (1975)
M. Gasperini, M. Giovannini, G. Veneziano, Phys. Rev. Lett. **75**, 3796 (1995)

M. Giovannini, K.E. Kunze, Phys. Rev. D **77**, 063003 (2008)
S.C.O. Glover, D.W. Savin, Mon. Not. R. Astron. Soc. **393**, 911 (2009)
N.Y. Gnedin, A. Ferrara, E.G. Zweibel, Astrophys. J. **539**, 505 (2000)
D. Grasso, H.R. Rubinstein, Phys. Rep. **248**, 163 (2001)
P.J. Greenberg, Astrophys. J. **164**, 589 (1971)
A.H. Guth, S.-Y. Pi, Phys. Rev. Lett. **49**, 1110 (1982)
S.W. Hawking, Phys. Lett. B **115**, 295 (1982)
P. Hennebelle, S. Fromang, Astron. Astrophys. **477**, 9 (2008)
P. Hennebelle, R. Teyssier, Astron. Astrophys. **477**, 25 (2008)
B. Himmetoglu, C.R. Contaldi, M. Peloso, Phys. Rev. Lett. **102**, 111301 (2009a)
B. Himmetoglu, C.R. Contaldi, M. Peloso, Phys. Rev. D **81**, 063528 (2009b)
C.J. Hogan, Phys. Rev. Lett. **51**, 1488 (1983)
F. Hoyle, in *Proceedings of the Symposium on Motion of Gaseous Masses of Cosmical Dimensions*, ed. by J.M. Burgers, H.C. van de Hulst (Central Air Documents Office, Dayton, 1949), p. 195
F. Hoyle, Nature **223**, 936 (1969)
K. Ichiki, K. Takahashi, H. Ohno, H. Hanayama, N. Sugiyama, Science **311**, 827 (2006)
K. Ichiki, K. Takahashi, N. Sugiyama, H. Hanayama, H. Ohno, astro-ph/0701329v1 (2006)
J.D. Jackson, *Classical Electrodynamics* (Wiley, New York, 1975)
K. Jedamzik, V. Katalinić, A.V. Olinto, Phys. Rev. D **57**, 3264 (1998)
K. Jedamzik, V. Katalinić, A.V. Olinto, Phys. Rev. Lett. **85**, 700 (2000)
T. Kahniashvili, B. Ratra, Phys. Rev. **71**, 103006 (2005)
A.J. Keane, R.K. Barrett, Class. Quantum Gravity **17**, 201 (2000)
K.-T. Kim, P.P. Kronber, G. Giovannini, T. Vernturi, Nature **341**, 720 (1989)
E.-J. Kim, A.V. Olinto, R. Rosner, Astrophys. J. **468**, 28 (1996)
E.W. Kolb, M.S. Turner, *The Early Universe, Frontiers in Physics* (Addison-Wesley, Reading, 1990)
E. Komatsu, K.M. Smith, J. Dunkley, C.L. Bennett, B. Gold, G. Hinshaw, N. Jarosik, D. Larson, M.R. Nolta, L. Page, D.N. Spergel, M. Halpern, R.S. Hill, A. Kogut, M. Limon, S.S. Meyer, N. Odegard, G.S. Tucker, J.L. Weiland, E. Wollack, E.L. Wright, arXiv:1001.4538 (2010)
A. Kosowsky, A. Loeb, Astrophys. J. **469**, 1 (1996)
P.P. Kronberg, Rep. Prog. Phys. **57**, 325 (1994)
P.P. Kronberg, Astrophys. J. **676**, 70 (2008)
P.P. Kronberg, J.P. Perry, E.L.H. Zukowski, Astrophys. J. **387**, 528 (1992)
R.M. Kulsrud, E.G. Zweibel, Rep. Prog. Phys. **71**, 046901 (2008)
R.M. Kulsrud, R. Cen, J.P. Ostriker, D. Ryu, Astrophys. J. **480**, 481 (1997)
M. Langer, J.-L. Puget, N. Aghanim, Phys. Rev. D **67**, 3505 (2003)
R.B. Larson, Mon. Not. R. Astron. Soc. **145**, 271 (1969)
A. Lazarian, Astron. Astrophys. **264**, 326 (1992)
A. Lewis, Phys. Rev. D **70**, 043011 (2004)
D.H. Lyth, A. Woszczyna, Phys. Rev. D **52**, 3338 (1995)
M.N. Machida, K. Omukai, T. Matsumoto, S. Inutsuka, Astrophys. J. Lett. **647**, L1 (2006)
A. Mack, T. Kahniashvili, A. Kosowsky, Phys. Rev. D **65**, 123004 (2002)
H. Maki, S. Hajime, Astrophys. J. **609**, 467 (2004)
J. Martin, J. Yokoyama, J. Cosmol. Astropart. Phys. **1**, 25 (2008)
St. Mrówczyński, Phys. Lett. B **214**, 587 (1988)
St. Mrówczyński, Phys. Lett. B **314**, 118 (1993)
A. Neronov, I. Vovk, Science **328**, 73 (2010)
J.A. Peacock, *Cosmological Physics* (Cambridge University Press, Cambridge, 1999)
P.J.E. Peebles, Astrophys. J. **155**, 393 (1969)
P.J.E. Peebles, *Principles of Physical Cosmology*. Princeton Series in Physics (Princeton University Press, Princeton, 1993)
M.V. Penston, Mon. Not. R. Astron. Soc. **144**, 425 (1969)
C. Pinto, D. Galli, Astron. Astrophys. **484**, 17 (2008)
C. Pinto, D. Galli, F. Bacciotti, Astron. Astrophys. **484**, 1 (2008)
Yu.E. Pokrovsky, A.V. Selikhov, Pis'ma Zh. Eksp. Teor. Fis. **47**, 11 (1988) [English Translation JETPL **47**, 12 (1988)]
R.E. Pudritz, J. Silk, Astrophys. J. **342**, 650 (1989)
J.A. Quashnock, A. Loeb, D. Spergel, Astrophys. J. Lett. **344**, L49 (1989)
B. Ratra, Astrophys. J. **391**, L1 (1992)
A. Rebhan, M. Strickland, M. Attems, Phys. Rev. D **78**, 045023 (2008)
M.J. Rees, Q. J. R. Astron. Soc. **28**, 197 (1987)
M.J. Rees, in *Cosmical Magnetism*, ed. by D. Lynden-Bell (Kluwer Academic, Dordrecht, 1994), p. 155

L.F.S. Rodrigues, R.S. de Souza, R. Opher, Mon. Not. R. Astron. Soc. **406**, 482 (2010)
P. Romatschke, A. Rebhan, Phys. Rev. Lett. **97**, 252301 (2006)
B. Schenke, A. Dumitru, Y. Nara, M. Strickland, J. Phys. G **35**, 104101 (2008)
D.R.G. Schleicher, D. Galli, F. Palla, M. Camenzind, R.S. Klessen, M. Bartelmann, S.C.O. Glover, Astron. Astrophys. **490**, 521 (2008)
D.R.G. Schleicher, R. Banerjee, R.S. Klessen, Astrophys. J. **692**, 236 (2009a)
D.R.G. Schleicher, D. Galli, S.C.O. Glover, R. Banerjee, F. Palla, R. Schneider, R.S. Klessen, Astrophys. J. **703**, 1096 (2009b)
D.R.G. Schleicher, Astron. Astrophys. arXiv:1008.3481 (2010)
S. Seager, D.D. Sasselov, D. Scott, Astrophys. J. Lett. **523**, L1 (1999)
T.R. Seshadri, K. Subramanian, Phys. Rev. Lett. **87**, 101301 (2001)
T.R. Seshadri, K. Subramanian, Phys. Rev. Lett. **103**, 081303 (2009)
S.K. Sethi, K. Subramanian, Mon. Not. R. Astron. Soc. **356**, 778 (2005)
S.K. Sethi, Z. Haiman, K. Pandey, arXiv:1005.2942 (2010)
J.R. Shaw, A. Lewis, Phys. Rev. D **81**, 043517 (2010)
G. Sigl, A.V. Olinto, K. Jedamski, Phys. Rev. D **55**, 4582 (1997)
J. Silk, Astrophys. J. **151**, 431 (1968)
J. Silk, M. Langer, Mon. Not. R. Astron. Soc. **371**, 444 (2006)
D.T. Son, Phys. Rev. D **59**, 063008 (1999)
A.A. Starobinskii, Phys. Lett. B **117**, 175 (1982)
H. Stefani, *Introduction to General Relativity* (Cambridge University Press, Cambridge, 1990)
M.A. Stenrup, A. Larson, N. Elander, Phys. Rev. A **79**, 012713 (2009)
M. Strickland, Braz. J. Phys. **37**, 762 (2007a)
M. Strickland, J. Phys. G, Nucl. Part. Phys. **34**, S429 (2007b)
K. Subramanian, Astron. Nachr. **327**, 333 (2006)
K. Subramanian, Mon. Not. R. Astron. Soc. **294**, 718 (1998)
K. Subramanian, Astron. Nachr. **331**, 110 (2010)
K. Subramanian, J.D. Barrow, Phys. Rev. D **58**, 083502 (1998)
K. Subramanian, J.D. Barrow, Phys. Rev. Lett. **81**, 3575 (1998)
K. Subramanian, D. Narasimha, S.M. Chitre, Mon. Not. R. Astron. Soc. **271**, 15 (1994)
K. Subramanian, T.R. Seshadri, J.D. Barrow, Mon. Not. R. Astron. Soc. **344**, L31 (2003)
S. Sur, et al., Astrophys. J. Lett. **721**, L134 (2010)
S.I. Syrovatskii, in *Interstellar Gas Dynamics*, ed. by H.J. Habbing. IAU Symposium No. 39 (Springer, New York, 1970)
K. Takahashi et al., Mon. Not. R. Astron. Soc. **410**, 247 (2011)
J.C. Tan, E.G. Blackman, Astrophys. J. **603**, 401 (2004)
H. Tashiro, N. Sugiyama, Mon. Not. R. Astron. Soc. **368**, 965 (2006a)
H. Tashiro, N. Sugiyama, Mon. Not. R. Astron. Soc. **372**, 1060 (2006b)
K. Thorne, Astrophys. J. **148**, 51 (1967)
C.G. Tsagas, Class. Quantum Gravity **22**, 393 (2005)
C.G. Tsagas, A. Kandus, Phys. Rev. D **71**, 123506 (2005)
C.G. Tsagas, A. Challinor, R. Maartens, Phys. Rep. **465**, 61 (2008)
M.S. Turner, L.M. Widrow, Phys. Rev. D **37**, 2743 (1988)
T. Vachaspati, Phys. Lett. B **265**, 258 (1991)
E. Weibel, Phys. Rev. Lett. **2**, 83 (1959)
S.D.M. White, Astrophys. J. **286**, 38 (1984)
L.M. Widrow, Rev. Mod. Phys. **74**, 775 (2002)
H. Xu et al., Astrophys. J. Lett. **688**, L57 (2008)
A. Yahil, Astrophys. J. **265**, 1047 (1983)
D.G. Yamazaki, K. Ichiki, T. Kajino, G.J. Mathews, Phys. Rev. D **77**, 043005 (2008)
Ya.B. Zel'dovich, Astron. Astrophys. **5**, 84 (1970)